INFORMATION TO USERS

This manuscript has been reproduced from the microfilm master. UMI films the text directly from the original or copy submitted. Thus, some thesis and dissertation copies are in typewriter face, while others may be from any type of computer printer.

The quality of this reproduction is dependent upon the quality of the copy submitted. Broken or indistinct print, colored or poor quality illustrations and photographs, print bleedthrough, substandard margins, and improper alignment can adversely affect reproduction.

In the unlikely event that the author did not send UMI a complete manuscript and there are missing pages, these will be noted. Also, if unauthorized copyright material had to be removed, a note will indicate the deletion.

Oversize materials (e.g., maps, drawings, charts) are reproduced by sectioning the original, beginning at the upper left-hand corner and continuing from left to right in equal sections with small overlaps. Each original is also photographed in one exposure and is included in reduced form at the back of the book.

Photographs included in the original manuscript have been reproduced xerographically in this copy. Higher quality 6" x 9" black and white photographic prints are available for any photographs or illustrations appearing in this copy for an additional charge. Contact UMI directly to order.

UMI

A Bell & Howell Information Company
300 North Zeeb Road, Ann Arbor MI 48106-1346 USA
313/761-4700 800/521-0600

Reproduced with permission of the copyright owner. Further reproduction prohibited without permission.

Reproduced with permission of the copyright owner. Further reproduction prohibited without permission.

NOTE TO USERS

The original manuscript received by UMI contains pages with indistinct print. Pages were microfilmed as received.

This reproduction is the best copy available

UMI

Reproduced with permission of the copyright owner. Further reproduction prohibited without permission.

Reproduced with permission of the copyright owner. Further reproduction prohibited without permission.

The Application of a Physically Based Hydrological Model on a Semi-Arid Watershed in Northern Ghana

by

Arnold Rudy ©

A Graduate Thesis Submitted
in Partial Fulfilment of the Requirements
for the Degree of Master of Science in Forestry

Faculty of Forestry
Lakehead University
Ontario, Canada

February, 1997

Reproduced with permission of the copyright owner. Further reproduction prohibited without permission.

National Library of Canada
Acquisitions and Bibliographic Services
395 Wellington Street
Ottawa ON K1A 0N4
Canada

Bibliothèque nationale du Canada
Acquisitions et services bibliographiques
395, rue Wellington
Ottawa ON K1A 0N4
Canada

Your file Votre référence

Our file Notre référence

The author has granted a non-exclusive licence allowing the National Library of Canada to reproduce, loan, distribute or sell copies of this thesis in microform, paper or electronic formats.

L'auteur a accordé une licence non exclusive permettant à la Bibliothèque nationale du Canada de reproduire, prêter, distribuer ou vendre des copies de cette thèse sous la forme de microfiche/film, de reproduction sur papier ou sur format électronique.

The author retains ownership of the copyright in this thesis. Neither the thesis nor substantial extracts from it may be printed or otherwise reproduced without the author's permission.

L'auteur conserve la propriété du droit d'auteur qui protège cette thèse. Ni la thèse ni des extraits substantiels de celle-ci ne doivent être imprimés ou autrement reproduits sans son autorisation.

0-612-33446-5

Canada

Reproduced with permission of the copyright owner. Further reproduction prohibited without permission.

ABSTRACT

Rudy, A. 1996. The Application of a Physically Based Hydrological Model on a Semi-Arid Watershed in Northern Ghana. MSc. (Forestry) Thesis. Faculty of Forestry, Lakehead University, Thunder Bay, Ontario, Canada. 94 pp. (Advisor: U.T. Runesson, PhD.)

Keywords: geographic information system, Ghana, landuse, physically distributed watershed modelling, remote sensing, semi-arid environment

Land degradation in semi-arid environments is increasing due to rapid population growth, poor landuse practices and variable climate conditions. Landuse planners require a better understanding of the impact that proposed changes in landuse practices have on a watershed's hydrologic response when implementing policies and programs designed to decrease the detrimental effects of land degradation. A physically based hydrological model, r.hydro.CASC2D, was used to illustrate the impact changes in landuse practices have on the hydrologic response of a semi-arid watershed located in northern Ghana. The development of the required model input parameters using geographical information systems and remote sensing technologies is described. A sensitivity analysis on selected model inputs was conducted. The models output was sensitive to all model input parameter tested, such as grid cell size, Green and Ampt soil infiltration parameters and Manning's n values. Two landuse scenarios were then developed to illustrate the impact of implementing landuse practices that increase vegetative ground cover. With increasing vegetative cover, peak discharges decreased with an associated delayed time to peak discharge. In addition, total runoff volume decreased as the level of vegetation increased, resulting in total volume of water infiltrating.

Reproduced with permission of the copyright owner. Further reproduction prohibited without permission.

LIBRARY RIGHTS STATEMENT

In presenting this thesis in partial fulfillment of the requirements for the degree of Master of Science in Forestry at Lakehead University at Thunder Bay, I agree that the University shall make it freely available for inspection.

This university thesis is made available by my authority for the purposes of academic study and research and may not be copied or reproduced in whole or in part (except as permitted by the Copyright Laws) without my written authority.

Signature_____

Date_____

Reproduced with permission of the copyright owner. Further reproduction prohibited without permission.

CONTENTS

ABSTRACT	ii
TABLES	vi
FIGURES	vii
ACKNOWLEDGEMENTS	ix
CHAPTER 1: OBJECTIVES AND SCOPE	1
CHAPTER 2: BACKGROUND INFORMATION	3
2.1 Hydrological Modelling	3
2.2 Geographic Information Systems	8
2.2.1 r.hydro.CASC2D	9
2.3 Satellite Remote Sensing	11
2.4 Environmental Degradation in Ghana	14
2.4.1 Environmental Policy	17
2.4.2 GIS and Remote Sensing Activities in Ghana	18
CHAPTER 3: STUDY AREA	20
CHAPTER 4: DATABASE	26
4.1 Purpose	26
4.2 General Database Compilation	27
4.3 Digital Elevation Model	28
4.4 Watershed Mask Grid	32
4.5 Infiltration Parameters Grid	36
4.6 Manning's n Value Grid	38
4.6.1 Image Rectification	39
4.6.2 Landuse Classification	40
4.7 Rainfall Event	44
4.8 Watershed Outlet Location and Slope and Computational Time Step	46
CHAPTER 5: PARAMETER SENSITIVITY ANALYSIS	47
5.1 Purpose	47
5.2 Sensitivity Analysis for Grid Cell Size	47
5.3 Sensitivity Analysis for Green and Ampt Infiltration Parameter	51
5.4 Sensitivity Analysis for Manning's n Overland Roughness Coefficient	57

Reproduced with permission of the copyright owner. Further reproduction prohibited without permission.

CHAPTER 6: LANDUSE SCENARIOS 60

6.1 Purpose 60
6.2 Landuse Scenarios 60
6.3 Model Calibration and Verification 67

CHAPTER 7: DISCUSSION 69

7.1 Database 69
7.2 Model Sensitivity 70
7.3 Landuse Scenarios 71
7.4 Study Limitations 73

CHAPTER 8: CONCLUSIONS AND RECOMMENDATIONS 74

8.1 Conclusions 74
8.2 Recommendations for Future Research 75

LITERATURE CITED 76

APPENDIX 1 82

APPENDIX 2 85

APPENDIX 3 92

Reproduced with permission of the copyright owner. Further reproduction prohibited without permission.

TABLES

Table		Page
2.1	Spectral and spatial image characteristics for Landsat Thematic Mapper (TM) and SPOT multisensor (XS) data	12
2.2	Cultivation treatment assigned to runoff plots	16
4.1	Required r.hydro.CASC2D parameter input maps for this study	26
4.2	Estimated Green and Ampt soil infiltration parameters	38
4.3	Landuse class codes and description	43
4.4	Summary of assigned Manning's n values and percentage of area for each landuse class	44
5.1	Summary of r.hydro.CASC2D input parameters for grid cell sensitivity simulations	48
5.2	Summary of r.hydro.CASC2D input parameters required for Green and Ampt soil infiltration sensitivity simulations	52
5.3	Estimated Green and Ampt soil infiltration parameters based on soil texture	54
5.4	Summary of model sensitivity to soil infiltration using various Green and Ampt parameters based on soil texture and initial soil moisture at 1/3 and 15 bar	55
5.5	Summary of r.hydro.CASC2D input parameters required for Manning's n sensitivity simulations	58
6.1	Percentage of watershed area of each landuse class and its associated change for each landuse scenario	64
6.2	Summary of r.hydro.CASC2D input parameters required for landuse scenarios	65
6.3	Summary results of landuse scenarios	66

Reproduced with permission of the copyright owner. Further reproduction prohibited without permission.

FIGURES

Figure		Page
3.1	Geographic location of study area	21
3.2	Soil map	22
3.3	Soil quality map	23
3.4	Average monthly rainfall and temperature data from the Bawku-Manga meteorological station for the 1960-1993 time period	24
4.1	GIS coverages generated from the 1:50,000 scale Ghana topographic map sheet	27
4.2	TOPOGRID input coverages	29
4.3	Gray shaded DEM generated with TOPOGRID	30
4.4	Flow chart of steps required to delineate watershed boundary	32
4.5	Possible flow direction codes assigned to cell x	32
4.6	Main roads	34
4.7	Watershed a) streams and b) contours	35
4.8	Soil quality	37
4.9	Dry season 1991 false color SPOT XS satellite image	41
4.10	Two band scatterplot in spectral space showing two possible clusters: water and vegetation	42
4.11	Landuse classes derived from dry season SPOT XS satellite image	45

Reproduced with permission of the copyright owner. Further reproduction prohibited without permission.

Figure Page

5.1 Summary of changes to watershed area, watershed perimeter, average slope, number of cells and spatial extent for three different cell sizes: 75 m, 100 m, 200 m 50

5.2 Hydrographs illustrating sensitivity to 75 m, 100 m and 200 m grid cell sizes 51

5.3 Hydrographs illustrating sensitivity to Green and Ampt soil infiltration parameters based on soil texture and initial soil moisture at 1/3 bar and 15 bar 56

5.4 Hydrographs illustrating sensitivity of Manning's n overland flow parameter 59

6.1 Landuse class distribution for Case 1 62

6.2 Landuse class distribution for Case 2 63

6.3 Hydrographs illustrating effect of different landuse scenarios 66

Reproduced with permission of the copyright owner. Further reproduction prohibited without permission.

ACKNOWLEDGEMENTS

I wish to thank my graduate advisor, Dr. Ulf Runesson (Faculty of Forestry) for his guidance, encouragement and friendship during my study period at Lakehead University and during our work periods in Ghana, West Africa. I would also like to extend my appreciation to my committee members, Dr. W. L. Meyer (Faculty of Forestry, Lakehead University) and Dr. James Quashie-Sam (IRNR-UST, Ghana) for their guidance and review of this thesis.

The successful completion of this thesis is also due to the contributions of the LU-CARIS computer facilities at Lakehead University and the Canadian International Development Agency (CIDA), which provided the satellite imagery needed for this study and provided the opportunity for my travel and work term in Ghana, West Africa.

I would also like to extend a special thanks to my parents and family who have encouraged and supported me throughout my studies at Lakehead University.

Arnold Rudy

Reproduced with permission of the copyright owner. Further reproduction prohibited without permission.

CHAPTER 1: OBJECTIVES AND SCOPE

The negative impact of poor landuse practices on a watershed's hydrology has long been recognized. Empirical studies have shown that poor landuse practices (*i.e.*, reduction of vegetation cover) affects both evapotranspiration and infiltration rates, and alters the quantity and distribution of surface runoff and stream discharge (Wu and Haith, 1993). This increases the potential for soil erosion, nutrient loss, stream channel modification and flooding (Sutherland, 1994). The impact of landuse on these hydrological processes may be further accentuated by climate conditions. In semi-arid environments this is of particular importance where a large portion of rain-fall is lost to surface runoff due to the short duration and high intensity of rainfall (Panda *et al.*, 1988). The impact of landuse on the magnitude and distribution of hydrological processes is often unknown.

For resource managers, identification and prediction of these changes can provide valuable information for use in short and long-term strategies involving flood control planning, irrigation, water conservation efforts and erosion control measures.

Objectives

The objectives of this study are intended to be a preliminary examination into:

1) the capabilities of a GIS integrated hydrological model, specifically r.hydro.CASC2D, in providing resource managers information on the hydrologic response of a watershed to changes in future landuse practices and patterns in a semi-arid environment;
2) the capabilities and limitations of remote sensing data in deriving and updating watershed characteristics for input into r.hydro.CASC2D; and
3) the extent to which model predictions are sensitive to changes in selected input parameters.

Reproduced with permission of the copyright owner. Further reproduction prohibited without permission.

The success of a hydrological model is dependent on the model's capability to simulate or predict the phenomena under study and the accuracy of input parameters. In the case of distributed parameter models, the amount of required input is large. The main thrust of this study is not concerned with the soundness of the selected model (Julien and Saghafian, 1991; Johnson *et al.*, 1993), but on the development of the GIS database required to run the model and its application in landuse planning.

The format of this document is as follows. Chapter 2 provides a review of literature on watershed modelling, background information on environmental degradation in Ghana, West Africa, and the role of geographical information systems (GIS) and remote sensing in watershed modelling. Chapter 3 provides a description of the study area located in the upper north east region of Ghana. Chapter 4 outlines the steps involved in compiling the model database. The results from a sensitivity analysis are given in Chapter 5. Chapter 6 provides general landuse scenario simulations followed by a discussion in Chapter 7. Conclusion and recommendations are presented in Chapter 8. Appendix 1 provides a listing of Green and Ampt soil infiltration parameters and Manning's n Values. Appendix 2 includes a description of the r.hydro.CASC2D command line. Appendix 3 illustrates the methodology followed in estimating the Green and Ampt infiltration parameters.

Reproduced with permission of the copyright owner. Further reproduction prohibited without permission.

CHAPTER 2: BACKGROUND INFORMATION

This chapter includes a brief literature review on watershed modelling, the role of geographical information systems (GIS) and remote sensing in physically based watershed modelling, and background information on environmental degradation in Ghana.

2.1 Hydrological Modelling

A variety of deterministic hydrological models exist that are capable of simulating and quantifying the various hydrological processes occurring within a watershed. The models range in structure, from simple lumped or "black-box" models which examine cause and effect (*i.e.*, relating rain-fall to surface runoff) relations within a watershed, to more complex distributed grid-based and physical based models that are based on the fundamental laws of physics, chemistry and biology (Becker and Serban, 1990).

Lumped models are generally applicable to real-time forecasting and approximating watershed discharge. They have the advantage of being easier to understand (and operate) and require a limited amount of input data. Their range of application is, however, limited to only gauged watersheds and typically require long-term historical data for calibration (Becker and Serban, 1990).

In contrast, distributed grid-based and physical-based models have a broader range of applications, including soil erosion, sediment transport and water quality studies. In addition, the impact of human activities, such as future landuse practices on hydrological processes, can be explored because model inputs have physical meaning and can be readily measured. Hydrologic responses, such as surface runoff, stream

Reproduced with permission of the copyright owner. Further reproduction prohibited without permission.

discharge, time to peak flow and sediment yield can be assessed under various rainfall events and landuse conditions. These models are also applicable to both gauged and ungauged watersheds. A major disadvantage is the requirement for detailed spatial data describing both watershed characteristics and climate data (Becker and Serban, 1990).

Distributed models allow input parameters to vary spatially over a watershed. The spatial variability of climate data and non-uniform watershed characteristics such as topography, soils, and landuse are taken into account. In comparison, lumped models treat the watershed as a homogenous unit in which input parameters are based on climate and watershed averages. Since lumped conceptual models are based on averages, the response of the watershed can only be evaluated at the outlet and processes occurring within the watershed cannot be calculated as they can be with distributed grid based models (Ponce, 1989).

The use of distributed grid-based and physical based models are growing in popularity compared to lumped models (Mazion, 1994). This change is reflected in the advances in computer technology (availability, capability), the integration of models with geographic information systems (GIS), availability of remote sensing data and improvements in the models themselves.

The time scale of the model is also an important factor. Time scales may be categorized as either single event or continuous. Single event models typically involve modelling the hydrologic response of a watershed based on a single rainfall event. Continuous models attempt to model the hydrology of the watershed over time, typically years (Haan *et al.*, 1994).

An important component in hydrological models is the accurate prediction of surface runoff. Transportation of pollutants and sediments are controlled by the surface runoff process. In general terms, the runoff process for a single rain-fall event describes water entering the watershed in the form of precipitation. The water is then either intercepted and/or absorbed by vegetation, retained on the surface, evaporated, infiltrated into the soil or once soil saturation has occurred, excess water may be removed as surface runoff into stream channels and routed downstream. In the distributed approach to single event modelling these processes are typically modelled as evapotranspiration,

Reproduced with permission of the copyright owner. Further reproduction prohibited without permission.

interception, and infiltration. Surface runoff is modelled as overland flow and channel routing. Evapotranspiration (ET), infiltration, and surface storage are collectively termed precipitation losses or abstractions because they represent precipitation that is lost to runoff.

Evapotranspiration in terms of hydrological modelling is the combined loss of moisture by evaporation (the change of state from liquid to vapour) and transpiration (loss of moisture from vegetation). Although ET may represent a large portion of precipitation losses on an annual basis, the rate of ET during a single rainstorm is small. Evapotranspiration losses are most significant between storms and less significant during a single rain event. For single event models, ET is often neglected (Haan *et al.*, 1994)..

Precipitation that adheres to surface vegetation and buildings is called interception, and is eventually lost through evaporation. Interception storage for a dense forest may equal 10 mm for a single rain event. Amounts vary depending on the surface conditions. During high intensity rain events, the amount of storage interception is low but may be significant over longer periods (Haan *et al.*, 1994). For modelling purposes, interception is often taken into account by subtracting the total interception storage from the incoming precipitation at the start of a rainfall event.

The flow of water into a soil is called infiltration and constitutes one of the most important precipitation losses (Haan *et al.*, 1994). The rate of infiltration is influenced by a variety of factors such as soil type, vegetation, antecedent moisture, slope and rainfall intensity. A coarse texture soil (sand) will usually have a greater infiltration rate than finer texture soils (clay) due to differences in pore sizes. A drier soil will have a higher infiltration rate compared to wetter soils. Therefore, for a given rain fall event, a dry soil will produce lower runoff rates than wetter soils. Generally, steeper slopes have a lower infiltration rate than flatter slopes. On steeper slopes, the time allowed for infiltration is lower because of the more rapid movement of water across the surface. High intensity rainfall may reduce the infiltration rate due to the impact of large raindrops onto the soil surface, which sometimes results in surface sealing. The effect of surface sealing can be reduced by adequate vegetation cover (Haan *et al.*, 1994).

Reproduced with permission of the copyright owner. Further reproduction prohibited without permission.

Water retained within surface depressions is called detention storage. The actual volume of water required to fill these depressions is called surface storage. Once surface storage capacity has been satisfied, surface runoff will occur. The determination of surface storage is difficult because it is dependent on slope and micro topography (Haan *et al.*, 1994).

Once precipitation losses have been accounted for, overland flow occurs to stream channels and moves downward as stream flow to the watershed outlet. In addition to surface runoff, stream flow includes sub-surface flow which moves laterally through the soil to the stream channel as groundwater or baseflow. Once within the stream channel, flow velocities and depths can be measured from which a hydrograph (graph of stream discharge over time) can be calculated.

For short intensity rain events where rainfall rates exceed the infiltration capacity of the soil, surface runoff is the most important component. Sub-surface and baseflow are often neglected in single event modelling.

Prediction of surface runoff usually employs the use of balance equations, such as the Saint Venant equations for shallow water flow (DeVantier and Feldman, 1993). When modelled in two-dimensional space, the balance equations take the form of second order partial differential equations and need to be solved by approximation methods (*e.g.*, finite difference methods or finite-element methods; DeVantier and Feldman, 1993). The theoretical background in modelling surface runoff is well documented in many hydrological books (Haan *et al.*, 1994; Bedient and Huber, 1992; and Ponce, 1989).

The Green and Ampt equation, which is based on Darcy's law of unsaturated flow in a porous medium, has been used extensively to simulate the soil infiltration process (James and Kim, 1990). The Green and Ampt equation is widely used over empirical based models, such as Horton's (1940) infiltration equation, because parameters are obtainable from measurable soil properties. The Green and Ampt equation takes the following form (from Saghafian, 1992):

$$f = K\left(1 + \frac{H_f M_d}{F}\right) \qquad \text{(Eqn. 1)}$$

Reproduced with permission of the copyright owner. Further reproduction prohibited without permission.

where f = infiltration rate

K = saturated hydraulic conductivity

H_f = capillary pressure head at the wetting front

M_d = soil moisture deficit $(\theta_e - \theta_i)$

θ_e = effective porosity equal to $(\phi - \theta_r)$

ϕ = total porosity

θ_r = residual saturation

θ_i = initial soil moisture content

F = total infiltrated depth

From Equation 1, three parameters are required to calculate the infiltration rate: K, H_f and M_d. Based on soil texture, Rawls *et al.* (1983a) have derived average values for K, H_f, θ_e and ϕ (see Appendix 1, Table A1.1). These values are commonly used when detailed soil infiltration data are unavailable. From Table A1.1, all of the required values can be obtained except for $M_d = (\theta_e - \theta_i)$ which varies according to rainfall conditions and moisture conditions. Total porosity is a measure of the proportion of pore space within a volume of soil and effective porosity accounts for the amount of air trapped within a volume of soil. Effective porosity is usually used in the Green and Ampt equation since it is a more reasonable value than total porosity. Hydraulic conductivity or permeability, is the rate at which water flows through soil under a unit potential energy gradient (Bedient and Huber, 1992).

Green and Ampt parameters have also been developed for soils under different soil tillage practices (Rawls *et al.*, 1983b). Based on known or estimated soil properties of percent sand and clay, organic matter and porosity change, Green and Ampt parameters, including soil moisture at field capacity (1/3 bar suction) and wilting point (15 bar suction), can be estimated from soil texture graphs. An additional correction factor may also be applied by reducing the saturated hydraulic conductivity for soils with an established surface crust (Brakensiek and Rawls, 1983).

Reproduced with permission of the copyright owner. Further reproduction prohibited without permission.

2.2 Geographic Information Systems

A geographic information system (GIS) is a digital system for managing, manipulating, analysing, displaying and mapping spatial data compiled or derived from existing maps, tables and reports, ground surveys, or remote sensing (*e.g.*, aerial photography or satellite imagery). Data can be stored in a raster (grid) or vector (point, arcs or polygons) format as maps (layers or coverage) containing specific geographic information.

GIS's use in hydrologic analysis have included: 1) deriving input parameters for existing hydrologic models; 2) displaying and mapping of hydrologic variables; 3) representing watershed surfaces; and 4) identifying hydrologic response units (Greene and Cruise, 1985).

Various lumped and physical-based hydrological models have been linked to different GIS platforms. The application of a GIS in conjunction with the U.S Army Corps of Engineer hydrologic model HEC-1 has been reported by Cline *et al.* (1989), and Suwanwerakamtorn (1994) who used various GIS software to derive HEC-1 model input parameters. Warwick and Haness (1994) tested the efficacy of a vector GIS (ARC/INFO) in deriving HEC-1 input parameters for a hypothetical watershed.

For raster based distributed modelling, Vieux and Gauer (1994) simulated storm water runoff using the Geographic Resource Analysis Support System (GRASS). GRASS is a public domain software package developed by the United States Army Corps of Engineers Construction Engineering Research Laboratory (CERL) as a general purpose grid-based geographic modelling and analysis package. Overland flow and channel routing was simulated using a finite-element and finite difference solution to the kinematic wave equation (a simplification of the Saint Venant equation). Data are entered manually or as raster maps describing each watershed's surface topography, infiltration, and soil hydraulic characteristics. Outputs consist of 1) hydrograph, which provide a continuous account of stream discharge over time; and 2) a set of distributed maps of flow rates which provide information on the source and magnitudes of surface

Reproduced with permission of the copyright owner. Further reproduction prohibited without permission.

runoff. A major limitation is its application to areas that have sufficient surface and channel relief (Vieux and Gauer, 1994).

GRASS has become a powerful public domain GIS system because source code and programming documentation is readily available which allows for the integration of programs for specific applications, including hydrological models developed in a non-GRASS environment (Wolfe and Neale, 1988)

Rewerts and Engel (1991) integrated GRASS and the Areal Nonpoint Source Watershed Environmental Response Simulation model (ANSWERS) developed by Beasley and Huggins (1981). The main application of ANSWERS is for erosion and sediment studies on lands used for agriculture. The ANSWERS program is a distributed model which simulates single event rainstorms. Engel *et al.* (1992) have integrated GRASS with the AGriculture NonPoint Source pollution model (AGNPS) developed by Young *et al.* (1987). The AGNPS program is a single event rainstorm model that is also appropriate for erosion and sediment studies. Savabi *et al.* (1995) discusses the application of deriving the needed input parameters using GRASS for the USDA-Water Erosion Prediction Project (WEPP).

2.2.1 r.hydro.CASC2D

Ogden and Saghafian (1996) developed a distributed hydrologic model fully integrated within GRASS capable of simulating the hydrologic response of a watershed for a given rainfall event called r.hydro.CASC2D. The major components of r.hydro.CASC2D include interception, infiltration and surface runoff routing. Infiltration is modelled using the Green and Ampt equation. Overland flow is modelled using a two dimensional finite difference technique while channel flow routing is modelled using one-dimensional explicit or implicit finite difference schemes.

A raster or grid format is utilized by r.hydro.CASC2D to represent the watershed spatial characteristics. Each raster consist of square grids which are assigned attributes describing a watershed characteristics (*e.g.*, infiltration parameter). Attributes are assumed to be homogenous across a grid element but may change from grid to grid. The grid cell resolution is controlled by the user and is dependent on the desired simulation

Reproduced with permission of the copyright owner. Further reproduction prohibited without permission.

accuracy, data accuracy and length of time required to run a simulation. Where detailed data are available, the selection of small grid sizes may be appropriate. For modelling of large watersheds, watersheds with a lack of detailed characteristics, or when simulation run times are high, larger grid sizes may be more appropriate (Julien, *et al.*, 1995).

Single event or multi-event rain storms using spatially uniform or spatially varied rainfall intensities may be modelled. Rainfall data may include rain gauge data from which rainfall intensities are spatially interpolated (*i.e.*, Thiessen polygon or inverse-distance square) or a time series of rainfall intensity maps. Time series maps may include radar maps or can be created from rain gauge data collected over time and interpolated into a time series of rainfall intensity maps.

Simulation of a single rainfall-runoff event is performed on each grid cell at each user defined computational time step. For each time step, rainfall is added to any existing surface water depth of a grid cell. The infiltration rate is calculated based on the soil characteristics. Any remaining surface water is then routed to the next grid cell according to the surface slope of surrounding grid cells. Excess water from overland grid cells that reach the channel are then routed through the channel network to the watershed outlet. Additional options allow for the accounting of baseflow, surface interception and storage by vegetation, soil moisture distribution for multi-storm events and depression storage. An earlier version of the model, known as CASC2D is documented in Julien and Saghafian (1991) and Saghafian (1992) and provide a description on some of the algorithms used in r.hydro.CASC2D. Subsurface flow and evapotranspiration are not considered in r.hydro.CASC2D.

The r.hydro.CASC2D model was specifically designed to utilize raster based input files, such as digital elevation models (DEM), landuse and land cover data, soil texture data and drainage networks.

Model outputs include: 1) discharge hydrographs at the watershed outlet and at specified internal watershed locations; and 2) raster maps at user defined time increments showing water surface depth, cumulative infiltration depth, surface soil moisture, infiltration rate and distributed rainfall intensity.

Reproduced with permission of the copyright owner. Further reproduction prohibited without permission.

The effects of large scale mechanized military maneuvers on the hydrologic response of a semi-arid watershed was examined by Doe (1992) using CASC2D and GRASS. Three hypothetical army maneuvers scenarios were simulated according to three different land management practices. Based on the level of maneuvers intensity, three levels of land disturbances (*i.e.*, none, medium, low) were derived. For each landuse disturbance, changes in soil hydrologic properties were also calculated. Each scenario was simulated and the temporal and spatial effects on discharge, infiltration depth and overland flow depths were examined.

2.3 Satellite Remote Sensing

The collection and analysis of data of a specific object or area, collected at a distance from a satellite or other methods is referred to as remote sensing . Remotely sensed data may be in the form of: 1) satellite imagery; 2) aerial photography; or 3) aerial imagery (ERDAS, 1991).

Two major sources of satellite data are supplied by the commercial Landsat and SPOT programs. Each satellite consists of a scanner with sensors made up of detectors calibrated to record reflected electromagnetic radiation as brightness values within specific regions of the electromagnetic spectrum. Within different regions of the electromagnetic spectrum, objects or features on the Earth's surface (*e.g.*, vegetation, soil and water) reflect electromagnetic radiation differently. This provides unique spectral signatures that allow for the identification of different features on an image.

The current Landsat 5 satellite contains a multispectral scanner (MSS) and a thematic scanner (TM). The SPOT satellite operates in a multispectral (XS) and panchromatic (PAN) mode. Both Landsat MSS and TM, and SPOT XS and PAN data contain different spectral and spatial characteristics. For example, Landsat TM data contains six reflective bands at a spatial resolution of 30 x 30 metres and one thermal band (6) with a spatial resolution of 120 x 120 metres. SPOT XS data have three spectral bands with a spatial resolution of 20 x 20 metres (Table 2.1).

Reproduced with permission of the copyright owner. Further reproduction prohibited without permission.

Table 2.1. Spectral and spatial image characteristics for Landsat Thematic Mapper (TM) and SPOT multisensor (XS) and panchromatic (PAN) data (adapted from ERDAS, 1991).

Sensor	Band	Spectral Resolution (μ)	Spatial Resolution (m)
Landsat	TM 1	0.45 - 0.52 (blue)	30 x 30
Landsat	TM 2	0.52 - 0.62 (green)	30 x 30
Landsat	TM 3	0.63 - 0.69 (red)	30 x 30
Landsat	TM 4	0.76 - 0.90 (near-infrared)	30 x 30
Landsat	TM 5	1.55 - 1.75 (middle-infrared)	30 x 30
Landsat	TM 6	10.4 - 12.5 (thermal)	120 x 120
Landsat	TM 7	2.08 to 2.35 (middle-infrared)	30 x 30
SPOT	XS 1	0.5 - 0.59 (green)	20 x 20
SPOT	XS 2	0.61 - 0.68 (red)	20 x 20
SPOT	XS 3	0.79 - .89 (near-infrared)	20 x 20
SPOT	Pan	0.51 - 0.73 (visible)	10 x 10

Remote sensing has been recognized as an important method for acquiring spatial input data required for hydrological models (Rango, 1985) and provides an effective means for up-dating existing resource information. For watersheds that are inaccessible, expand beyond international boundaries, or cover large geographic regions, remote sensing may be the only method for acquiring input data (Rango, 1985).

An extensive review of remote sensing techniques and its role in hydrology is presented by Kuittinen (1992). Uses and limitations of deriving information for hydrological studies on precipitation, soil moisture and groundwater, evapotranspiration, snow, ice and frost, surface water and watershed characteristics are discussed. Watershed characteristics mapped from remote sensing data include, topography, water courses, landuse/land cover, soil types and bedrock (Kuittinen, 1992).

Reproduced with permission of the copyright owner. Further reproduction prohibited without permission.

A common use of remote sensing data has been for deriving landuse/land cover maps for hydrological models. The majority of use has been directed at estimating the curve number utilizing landuse and land cover information for use in the Soil Conservation Service runoff Curve Number model (SCSCN) (Hill *et al.* 1987; White, 1988; and Stuebe and Johnston, 1990). The SCSCN model predicts potential surface runoff for use in stream flow and flood studies. Curve numbers are a function of landuse, soil characteristics and antecedent soil moisture.

In the distributed approach to surface flow, AGNPS, ANSWERS and r.hydro.CASC2D requires an input value describing a surface's resistance to surface flow, known as Manning's n roughness coefficient. Manning's n values have been derived for a variety of surfaces as shown in Table A.1.2 in Appendix 1. Information obtained from landuse/land class maps or from classified satellite imagery can be used to derive the appropriate value for the area under study.

A common list of landuse/land cover classes useful in hydrologic modelling derived from remote sensing data include: vegetation cover and types, cultivated areas, drainage, swamps and urban areas (Kuittinen, 1992).

Connors *et al.* (1985) used simulated SPOT data to discriminate areas of different hydrologic properties in semi-arid and humid regions by means of a variety of image analysis techniques. Hydrologic properties investigated included, infiltration rate, runoff rate, landscape stability, and wind and water erosion. For the semi-arid site, three surface classes based on infiltration rate, vegetation cover, soil texture, topography, and antecedent moisture were separated. The separated classes where as follows:

1) low infiltration rates (9.7 cm/hr) , well vegetated, fine grained soil, level topography with wet surface areas;
2) moderate infiltration rate, moderately vegetated, medium grained soil, hummocky, dry and intermediate surface areas; and
3) high infiltration (27 cm/hr), moderately well vegetated, coarse grained soil with relatively smooth, dry upland surface areas.

Based on vegetation cover, soil texture, salt content and micro topography obtained from remotely sensed data and additional information of general topography,

Reproduced with permission of the copyright owner. Further reproduction prohibited without permission.

landscape position and geomorphology areas of relative runoff rates (*i.e.*, low, moderate on high) were also identified.

2.4 Environmental Degradation in Ghana

Socio-economic and physical conditions are two factors linked to the continuing problem of environmental degradation in developing countries, such as Ghana. Rapid population growth (estimated at 3% per annum for 1987-2000 time period; UN, 1991), poor landuse practices (*i.e.*, reduced fallow periods, over-grazing, indiscriminate fuel wood harvesting, bush burning), and erratic climate conditions have contributed to the problem of environmental degradation in Ghana. Within the Upper North East Sudan Savanna region in Ghana, environmental degradation has reduced vegetation, increased soil erosion, lowered biodiversity and reduced soil fertility.

Environmental degradation increases the susceptibility of a region to drought and desertification and threatens long term environmental sustainability. In 1983, crop failure due to severe climatic conditions and improper landuse practices caused food shortages and famine throughout Ghana (Ofori-Sarpong, 1986). Desertification occurs when a land's biological productive capacity is destroyed. Although there are no areas of Ghana classified as desertified, 35% of the country is at risk of desertification (Dept. of Geography, 1992). Desertification is increasing within the savanna regions of Ghana (UN, 1991). The total cost of environmental degradation in Ghana for 1988 was estimated at four percent (US $128.3 million) of Ghana's gross domestic product. Cost of environmental degradation in 1988 from both agriculture and forestry activities was estimated at US $121.9 million (UN, 1991).

Loss of vegetation is one of the more important forms of environmental degradation in Ghana because it predisposes arable lands to further degradation, such as soil erosion. Adequate vegetation cover helps reduce soil erosion by intercepting and dissipating the energy in raindrops before it reaches the soil. Vegetation cover also helps to dissipate the energy of surface runoff and helps to encourage water infiltration into the soil (Pimentel, 1993).

Reproduced with permission of the copyright owner. Further reproduction prohibited without permission.

The primary effect of soil erosion is the reduction of on-site soil water storage within the plant rooting zone, which results from the gradual removal of organic matter, clay and soil colloids (Pimentel, 1993). In northern Ghana, eroded sites lose a substantial amount of water to surface runoff because of soil compaction and crusting, and from the short duration and high intensity rainfall in this region (Pimentel, 1993).

Bonsu and Obeng (1979) investigated the effect of various agriculture practices on soil degradation at the Manga Agriculture Station located in the Upper North East Region of Ghana. Ten rainfall runoff plots, each treated with a different cultivation method were measured for runoff, growth rates, crop yield, soil water losses, nutrient losses and the effect of grazing (Table 2.2). Grazing was found to increase soil loss by a factor of 1.8 compared to the ungrazed plot. They concluded that ridging across the slope, mulching and compound farming were the best cultivation practices for minimizing soil erosion.

Reproduced with permission of the copyright owner. Further reproduction prohibited without permission.

Table 2.2. Cultivation treatment assigned to runoff plots (from Bonsu and Obeng,1979).

Plot	Cultivation Treatment
1	Ridging across the slope: early millet and guinea corn interplanted with ground nuts and Bambara with no application of fertilizer.
2	Ridging across the slope: early millet and guinea corn interplanted with ground nuts and Bambara with an application of farm yard manure.
3	Mechanical tillage (hand operated rotators): early millet and guinea corn rotated with groundnuts and an application of fertilizer.
4	Ridging across the slope: early millet and guinea corn rotated with groundnuts and fertilized.
5	Mechanical tillage with straw mulching: early millet and guinea corn rotated with groundnuts and fertilized
6	Mechanical tillage: early millet and guinea corn rotated with groundnuts and fertilized
7	Mechanical tillage: guinea corn interplanted with early millet and fertilized.
8	Bare plot: control
9	Grazed: grass (*Andropogon gavanus*)/legume (*Styloxanthes humilis*) mixture with application of fertilizer.
10	No grazing: grass (*Andropogon gayanus*)/legume (*Styloxanthes humilis*) mixture with application of fertilizer.

Reproduced with permission of the copyright owner. Further reproduction prohibited without permission.

2.4.1 Environmental Policy

The government of Ghana has recognized the need to adopt and implement policies and programs which will move Ghana in the direction of sustainable development that will satisfy the present and future needs of the population and yet maintain sound environmental management of natural resources (Kendie, 1995).

Principles adopted by the government of Ghana to help secure sustainable development are outlined in the Environmental Action Plan (EAP). Approximately fifty projects are planned to be implemented by various national agencies through the EAP between 1991 and 2000. The Land Research Management Project, for example, was proposed to identify methods for improving land resource management in the Upper East Region (Dept. of Geography, 1992). In addition, the National Environmental Policy (NEP) was adopted as a framework for the implementation of the EAP (UN, 1991).

Specific aims of the NEP (UN, 1991) are to:

1) maintain ecosystems and ecological processes which are essential for the functioning of the biosphere;

2) ensure the sound management of natural resources and the environment; adequately protect humans, animals and plants, their biological communities and habitats, against harmful impacts and destructive practices, and preserve biological diversity;

3) guide development in accordance with quality requirements to prevent, reduce, and as far as possible, eliminate pollution and nuisances;

4) integrate environmental consideration in sectoral structures variable climate and socio-economic planning at the national, regional, district, and grassroots levels;

5) seek common solutions to environmental problems in West Africa, Africa, and the world at large.

The EAP clearly defines the need for sound environmental information. However, accurate, complete and up-to-date information is often lacking, which has

Reproduced with permission of the copyright owner. Further reproduction prohibited without permission.

hindered resource planning and decision making in Ghana (Issaka, 1992). In the case of implementing erosion control measures, which may involve alteration of landuse patterns for example, information on the hydrologic response of a watershed to control measures is often absent or not clearly understood.

2.4.2 GIS and Remote Sensing Activities in Ghana

A variety of GIS and remote sensing activities have been implemented in Ghana. Activities include developing suitability databases and maps for agriculture, water quality, and fish sensitivity assessment maps (Amoyaw-Osei, 1992), assessing land degradation in northern Ghana (Gyamfi-Aidoo 1987) and mapping airborne pollution (Danso, 1992).

Satellite imagery has been used to:

1) develop landuse and land cover maps for the Upper East Region (Department of Geography, 1992);
2) evaluate landuse change and hydrologic response of the Tamne watershed (Bulley, 1996);
3) identify and classify inland valleys (Amamoo-Otchere, 1990); and
4) produce forest inventory within Ghana's High Forest zone (Agurgo, 1992)

Image analysis, GIS and Global Positioning System (GPS) technologies have been used to develop landuse maps for selected pilot areas in northern Ghana under the Ghana Environmental Management Literacy Project (GEMLP) funded by the Canadian International Development Agency (CIDA). In addition the GEMLP program has setup workshops for training resource managers and faculty members in GIS, GPS and remote sensing technologies at the University of Science and Technology, Institute of Renewable Natural Resources in Kumasi.

Two country wide database building projects are currently being conducted. The first is based on Landsat TM data which will be used to produce 1:250,000 scale landuse maps. The second effort's aim is to convert the 1:50,000 Ghana Survey map sheets into a standardized digital database. Additionally, new digital databases are being developed

Reproduced with permission of the copyright owner. Further reproduction prohibited without permission.

from current aerial photography covering all major urban areas (Runesson, pers. comm., 1996).

Reproduced with permission of the copyright owner. Further reproduction prohibited without permission.

CHAPTER 3: STUDY AREA

The watershed selected for this study is located within the Upper East region of Ghana stretching between the latitudes of 0° 14' W and 0° 12' W and longitudes of 11° 01' N and 11° 07' N (Figure 3.1). The study watershed falls within the larger Nahau-Kulupielegu drainage basin. The main river within the study watershed flows northward into the east flowing Kulupielegu river. During the dry season months, flow within the watershed's main river ceases. No stream gauges exist within the watershed. Topography is of relatively low relief with an average slope of 1.5%. The watershed selected for this study was based on conversation with experienced field personnel working within the area who identified this area as being highly degraded.

Soils within the area are derived primarily from Granites with some alluvial based soil complexes in areas surrounding the Kulupielegu river. Based on a formal soil survey conducted by the Soil Research Institute of Ghana for the Navrongo-Bawku Area by Adu (1969), four soil associations and one soil complex were defined (Figure 3.2). Soil quality ranges from moderately deep, well drained fertile soils to very shallow, easily erodable soils of low fertility with low infiltration rates and high surface runoff (Figure 3.3).

Total annual rainfall amounts within the area are highly variable. Meteorological data from the Bawku-Manga Agriculture station shows total annual rainfall fluctuates from 1,311 mm/yr in 1973 to 598 mm/yr in 1983. Mean annual rainfall for the 1960 to 1993 time period was 915 mm/yr. Mean monthly rainfall and temperature data from the Bawku-Manga meteorological recording station are shown in Figure 3.4. A distinct dry season occurs between November and February where average monthly rainfalls are less than 9 mm with a monthly maximum of 450 mm occurring in August. Rainfalls are typically of short duration and of high intensity. For short time periods, rainfall

Reproduced with permission of the copyright owner. Further reproduction prohibited without permission.

Reproduced with permission of the copyright owner. Further reproduction prohibited without permission.

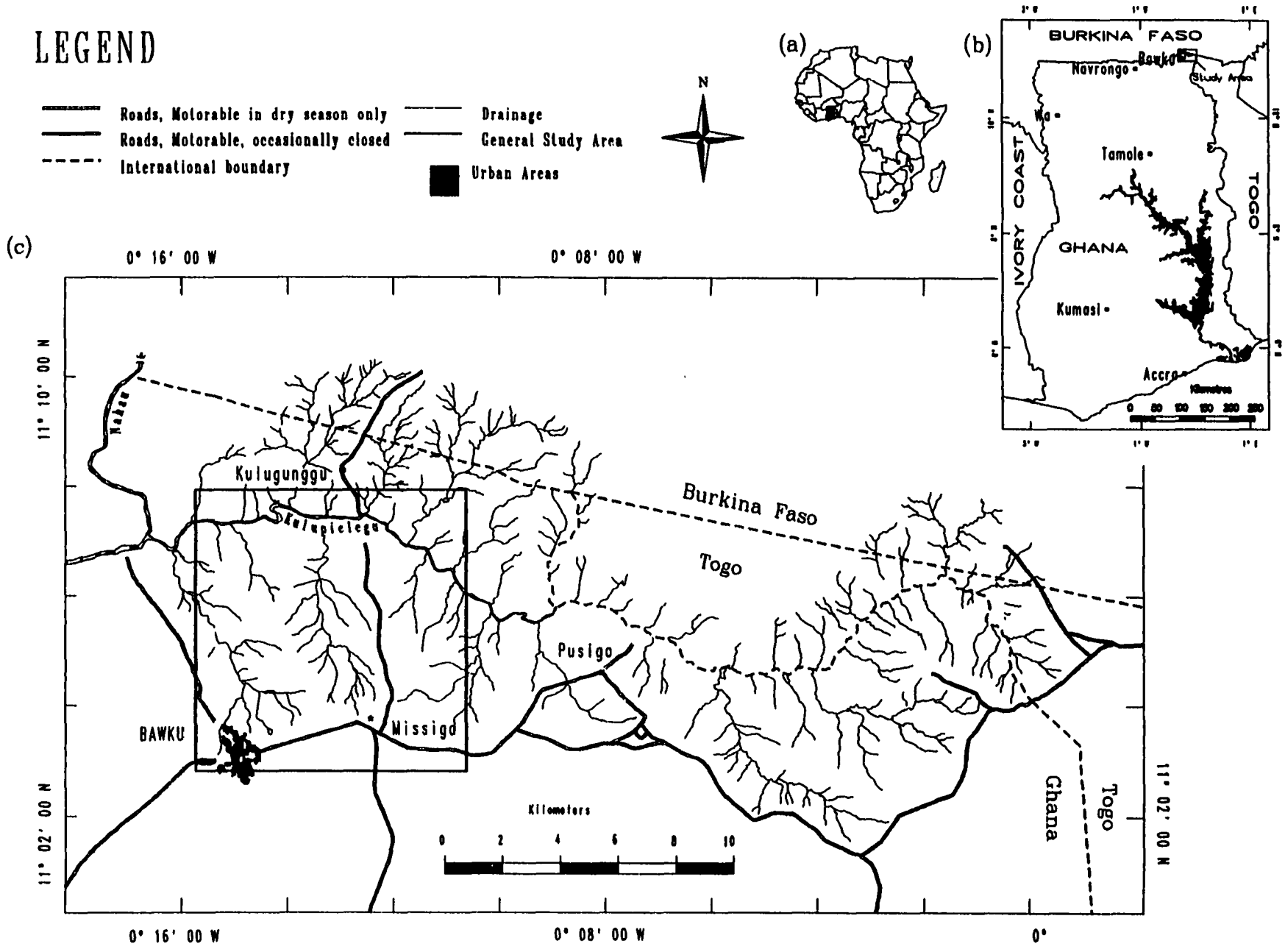

Figure 3.1. Geographic location of study watershed a) Africa b) Ghana c) North East Ghana.

Reproduced with permission of the copyright owner. Further reproduction prohibited without permission.

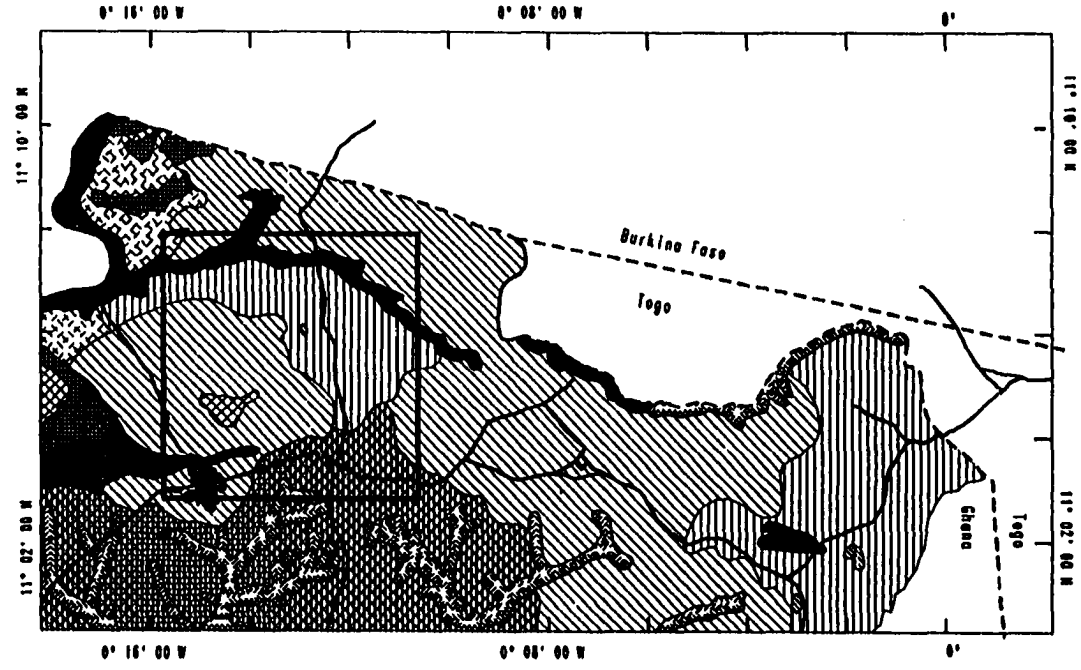

LEGEND

- Varempere (developed over Granites) Red and brown sandy loams and clays associated with hornblende granites; grey sandy loams and clays in valleys
- Yanchera association (developed over Granites) Moderately deep, pale brown coarse sandy loams associated with biotite granites; grey sandy loams and clays in valleys
- Puniga association (developed over Granites) Severly eroded soils developed over biotite granites, very shallow pale brown or greyish yellow weathered granite, highly feldspathic, very hard, compact, frequent rock outcrops, grey sandy loams and clays in valleys
- Chuchuliga association (developed over Granites) Granitic lithosols, mainly rock outcrops on high grounds, includes quartz reefs
- Nenchi association (developed over Granites) Massive boulders of ironpan capping summits of low tabular hills
- Kupelo-Bereniyase (developed over Granites) Grey sandy clays and loams in valley bottoms
- Voga association (soils developed over Birrimian rocks) Rocky lithosols, mainly greenstones, andesites, schists and amphibolite occurring on upper slopes and summits of hills
- Yagba association (soils developed over Birrimian rocks) Deep greyish yellow heavy calcareous clays derived from greenstones, andesites, schists and amphibolites, occurs on piedmont slopes, very dark grey clays in valley bottoms
- Nangodi association (soils developed over Birrimian rocks) Very stony soils derived from greenstones, andesites, schists and amphibolitesoccurring on lower to middle slopes of hills; olive grey or very dark grey clays on valley slopes and in bottoms
- Dagare association (soils derived from recent and old alluvia) River levees consisting of loose coarse sands and silty loams
- Siare-Pani association (soils derived from recent and old alluvia) Old flood-plain alluvium consisting of yellowish grey and very dark clacareous clays
- Siare-Dagare complex This comprises soils occurring in the Siare-Pani and Dagare association's not seperated on map
- Urban Area

- International Boundary
- Roads
- General Study Area

N

Kilometers

0 2 4 6 8 10

Figure 32. Soils map (adapted from Adu, 1969)

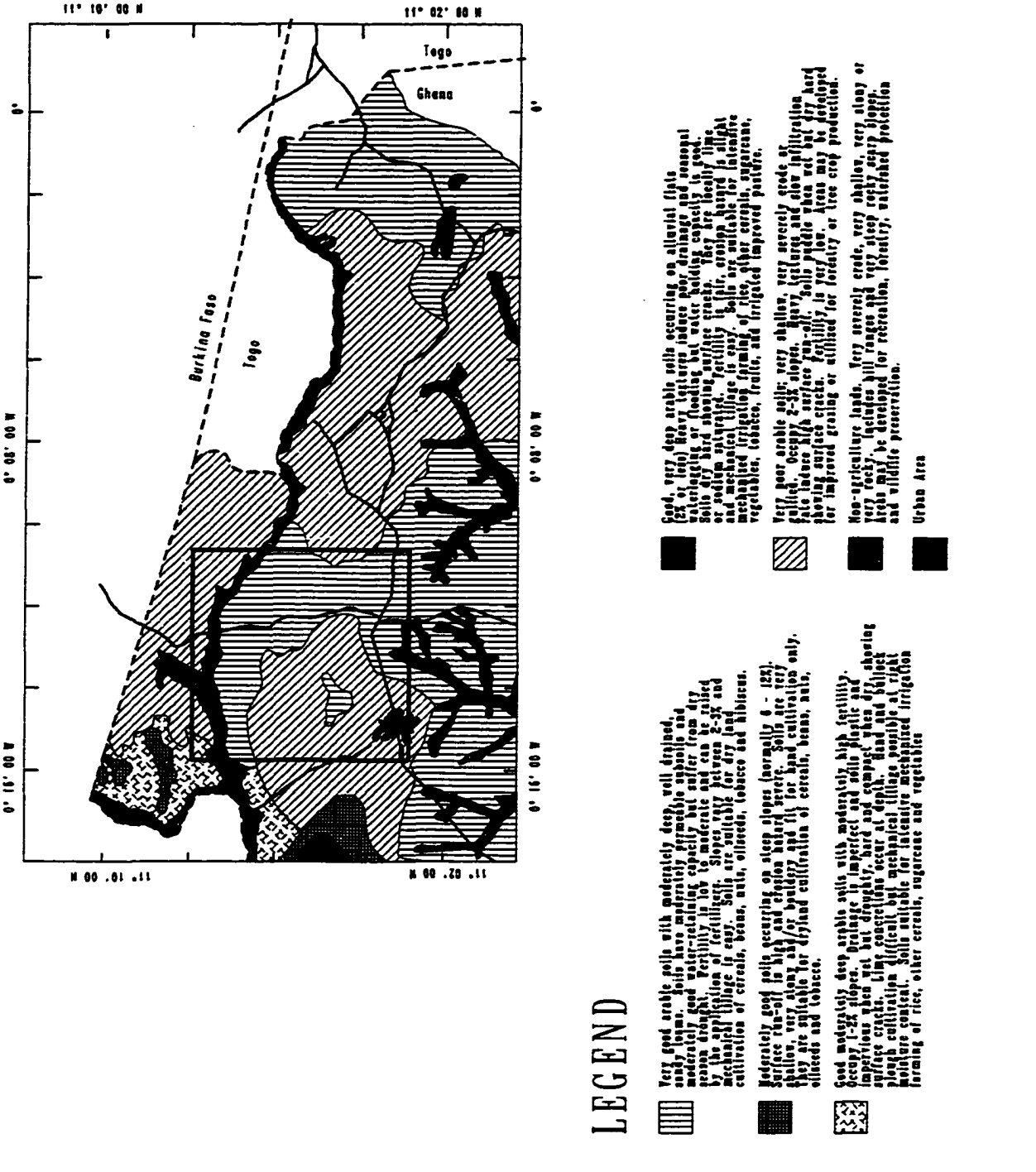

Figure 33. Soil quality map (adapted from Adu, 1964)

Reproduced with permission of the copyright owner. Further reproduction prohibited without permission.

intensities of 203 mm/hr are not uncommon (Adu, 1969). Mean monthly temperatures for the 1960-1993 time period shows minimal monthly temperature variation, with annual temperatures ranging from 27 to 32 °C (Figure 3.4).

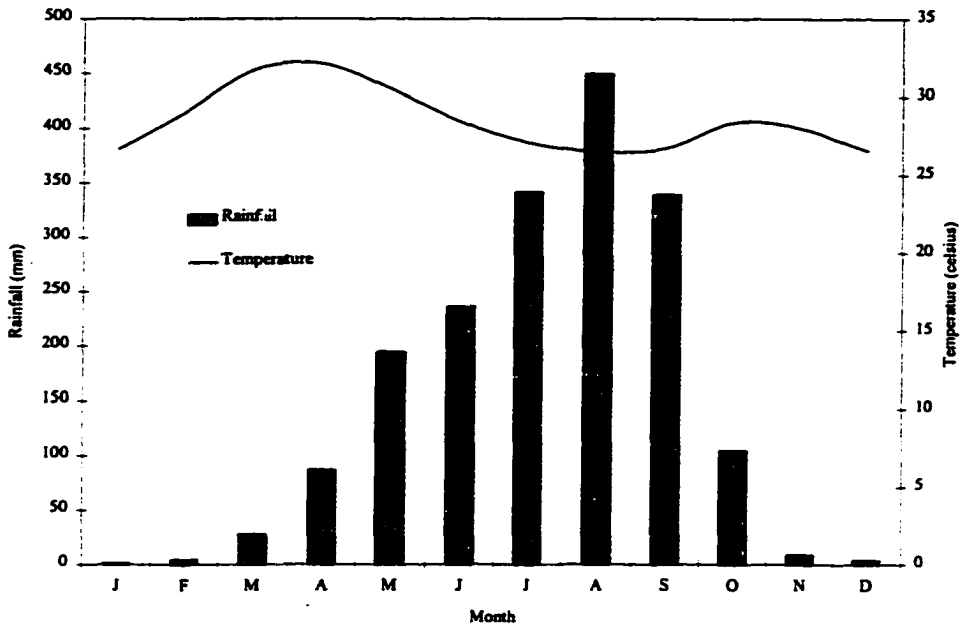

Figure 3.4. Average monthly rainfall and temperature data from the Bawku-Manga meteorological station for the 1960-1993 time period (Ghana Meteorological Services Department).

The timing and length of the rainy season is controlled by the location of the Inter-Tropical Discontinuity (ITD) boundary which separates the warm dry air mass (harmattan) originating from the Sahara desert and the moist warmer air mass (monsoon) originating from the South Atlantic Ocean. In January, one of the area's driest months, the area is influenced by the harmattan winds when the location of the ITD is between 5° and 7° N. In contrast, during the wetter summer months, the ITD moves northward (*i.e.*, to 20° N) and the study area becomes influenced by moist monsoon winds (Ofori-Sarpong, 1986).

The watershed falls within the Sudan savanna physiographic region which is characterized by low grass with scattered acacia (*Acacia albida* Del.), baobab trees (*Adansonia digitata* L.) and sheabutter trees (*Vitellaria paradoxa* Gaertn. f.).

Reproduced with permission of the copyright owner. Further reproduction prohibited without permission.

Landuse in the region is primarily directed towards agriculture which is dependent on the arrival and duration of the annual rains. Delay in the onset of the rains or if early rains are followed by dry periods, total or partial crop failure may result (Ofori-Sarpong, 1985).

A reconnaissance visit was made to the study area in August, 1995 with the purpose of gathering qualitative data on general landuse conditions and watershed characteristics. Observations made during the site visit with regards to landuse conditions and hydrologic conditions are summarized below.

1) Principal agriculture and cash crops grown in the area, without irrigation, are millet (*Pennisetum* spp.), maize (*Zea mays* L.), guinea-corn (*Sorghum bicolor* Moench), yam (*Dioscorea rotundata* Poir), groundnuts (*Arachis hypogaea* L.) and beans (various species).
2) Agriculture fields were intensively weeded and mainly cultivated by hand and hoe.
3) Open grazing of cattle was observed throughout the area. Overgrazing of cattle is a major problem within the area and contributes to the problem of land degradation through the removal of surface ground cover and compaction of soil.
4) Areas outside the cultivated fields are generally crusted, eroded soils with little vegetative cover. The boundary between the eroded and cultivated soils are very distinct.
5) Many of the streams are narrow but deeply incised with severe stream bank erosion occurring.
6) Rainfall events that occurred during the visit were typically of short duration, (less than two hours) but with high rainfall intensity. Surface runoff was rapid after each rainfall despite the low relief of the area.
7) Crusted soil surface conditions are a major factor controlling soil infiltration and surface runoff.

Reproduced with permission of the copyright owner. Further reproduction prohibited without permission.

CHAPTER 4: DATABASE

4.1 Purpose

This chapter outlines the procedures used in the generation, organization, manipulation and merging of the required model inputs. All relevant input data was compiled from existing soil and topographical maps, meteorological records, published data, limited field observations and satellite imagery.

Input data maps required for this study are presented in Table 4.1. Additional input parameters include location and slope of watershed outlet, rainfall duration, rainfall intensity and computational time step. Generation and formatting of inputs are discussed in detail in later sections. Saghafian and Ogden (1996) provide a complete description on data input, options and format requirements.

Table 4.1. Required r.hydro.CASC2D parameter input maps for this study.

Model Input Parameters (raster maps)	
Topography	Digital elevation model
Infiltration	Saturated hydraulic conductivity Capillary pressure head at the wetting front Effective porosity Initial moisture soil moisture
Overland Flow	Manning's n roughness values Watershed boundary mask

Reproduced with permission of the copyright owner. Further reproduction prohibited without permission.

The r.hydro.CASC2D model is executed within GRASS. Model inputs are entered at the command level or in an interactive mode which prompts the user for model inputs. To activate a specific model component (i.e., Green and Ampt infiltration and/or channel routing) the required input files are specified as input into r.hydro.CASC2D. The complete command line structure is presented in Appendix 2.

For the model, raster input maps are required to be in an integer format (non-decimal values); therefore, a fixed scaling factor is applied to all floating point values. All values presented are un-scaled values.

4.2 General Database Compilation

Topographical features, such as streams, roads, contours (15.24 m intervals), political boundaries, and major town locations were digitized from a 1:50,000 scale Survey of Ghana Topographical map sheet. Each feature (*e.g.*, roads) was stored as a separate coverage and attribute data was then assigned to each feature and stored in a relational database (Figure 4.1).

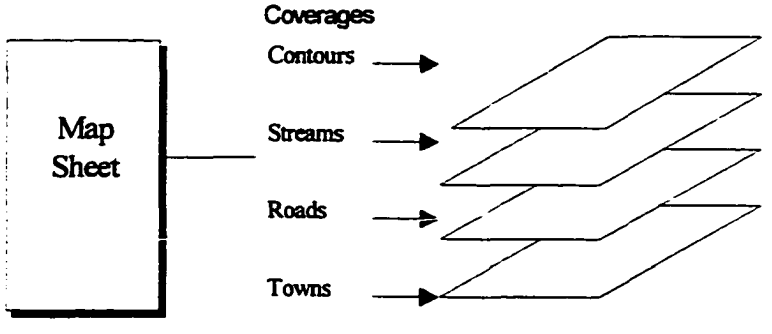

Figure 4.1. GIS coverages generated from the 1:50,000 scale Ghana topographic map sheet.

Ghana Survey maps use a Transverse Mercator projection system measured in feet. During the digitizing process, the x, y coverage coordinates were stored in digitizing units (*i.e.*, inches). A transformation was required which converted each coverage from digitizing units (inches) to the Transverse Mercator's projection coordinate system (feet). The accuracy of the transformation is expressed by the root

Reproduced with permission of the copyright owner. Further reproduction prohibited without permission.

mean square error (RMS) that describes the error between the original and new transformed coordinate location (ESRI, 1992). High RMS errors may result from digitizing errors, errors inherent in the source data or distortion in paper map sheets due to shrinking and stretching. The calculated transformation RMS error was 1.2 m.

4.3 Digital Elevation Model

One of the most important inputs into a distributed hydrological model is the Digital Elevation Model (DEM). A DEM is a regular array of numbers, usually representing elevation heights of the Earth's surface. Digital elevation model's generally take the form as either: a) contour based networks; b) triangular irregular networks; or c) regular square or grid networks. Due to their computational efficiency and compatibility with satellite imagery, regular grid networks are the most common DEM's in use (Moore *et al.*, 1991). Since contour based networks represent an irregular network of elevation data, interpolation is required to produce a continuous or regular grid of elevations (Mackey *et al.*, 1994).

A DEM of regular square grid cells was produced from contour and stream data using ARC/INFO's TOPOGRID program. The TOPOGRID program was specifically designed to produce hydrologically correct DEM's from point and/or contour data and stream data, and is based on Hutchinson's (1988) ANUDEM program.

The TOPOGRID program requires all streams to be represented by a single arc (line) and stream arcs must be orientated in a downstream direction and connected. During the digitizing process, the Kulupielegu river was digitized as a braided stream comprising of two arcs which define the outer boundary of the channel. Editing consisted of re-digitizing a single arc down the center of the channel, extending all branching streams to connect with the new channel arc and removing the channel boundary arcs. In order to ensure continuity in the stream coverage, polygons representing dam impoundments were removed and an arc was added connecting the beginning and end of the impounded area. All arcs orientated upstream were identified and re-orientated in a downstream direction (Figure 4.2).

Reproduced with permission of the copyright owner. Further reproduction prohibited without permission.

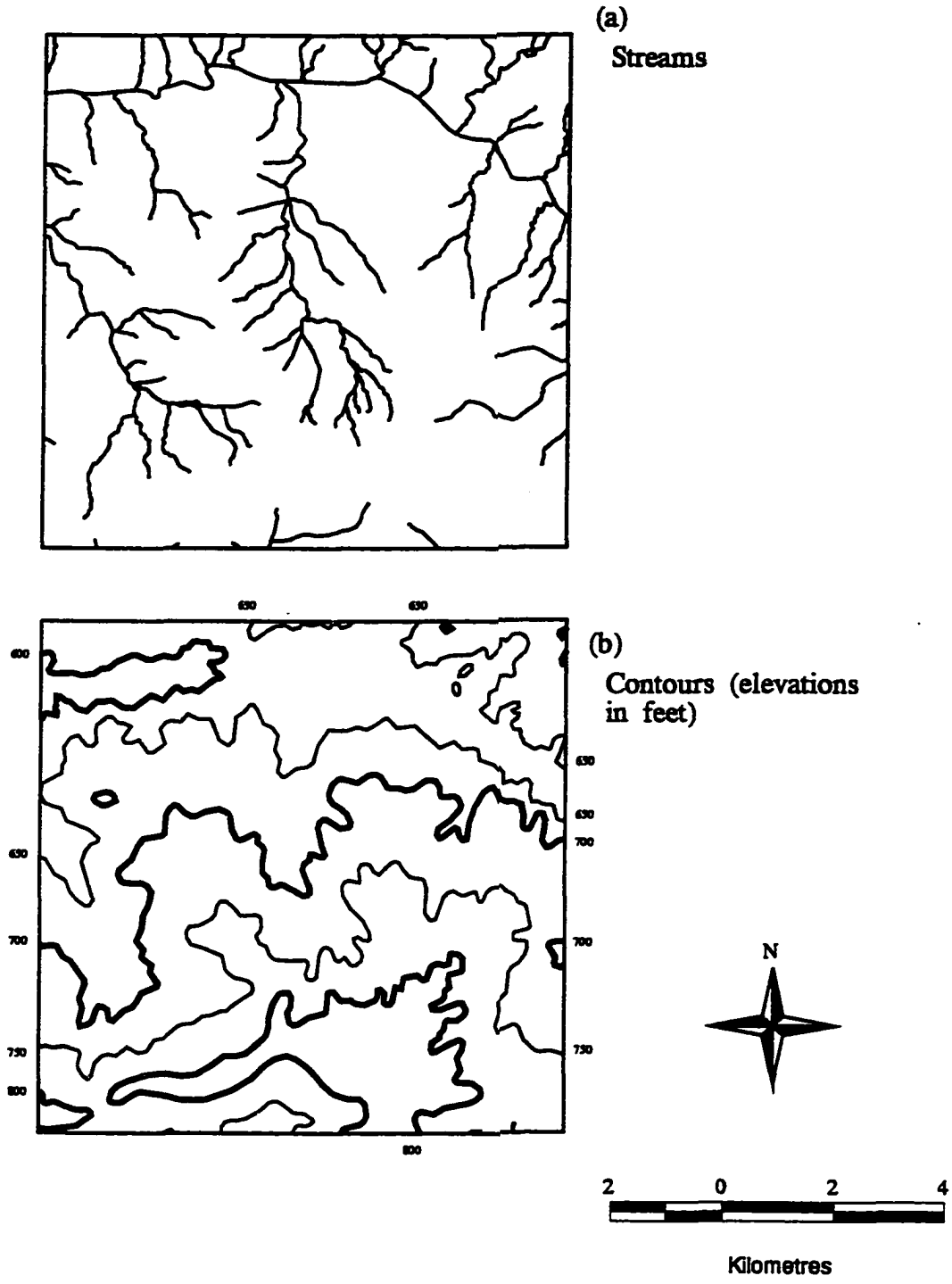

Figure 4.2. TOPOGRID input coverages a) streams b) contours (elevations in feet).

Reproduced with permission of the copyright owner. Further reproduction prohibited without permission.

Initially, numerous DEM's were produced at a 75 m grid cell resolution using various sets of three user-supplied elevation tolerances required during the drainage enforcement process. Tolerances selected were based on the level of surface generalization required and the resolution of input data (Hutchinson, 1989). Drainage enforcement, coupled with stream data, attempted to remove all unwanted sinks (depressions) and allowed for a more realistic drainage pattern within the fitted surface.

For each DEM generated, several diagnostic files were created to help evaluate the quality of the DEM's and input data. Diagnostic outputs included a point coverage showing remaining sinks not resolved by TOPOGRID. A line coverage of stream and ridge lines (localized surface maximums) which described the general morphology of the surface and an ASCII diagnostic file listed all specified input data and parameters, and listed the number of sinks removed.

Each DEM was evaluated in several ways:

1) A new contour coverage at half the original contour interval (12.5 m) was created from the DEM and overlaid onto the original contour data and visually compared;
2) The diagnostic drainage coverage was overlaid onto the original stream data and visually compared, and;
3) The diagnostic sink coverage was overlaid onto the original contour and stream data to determine the locations of remaining sinks.

A DEM that best matched the contour and stream data was then selected (Figure 4.3).

Reproduced with permission of the copyright owner. Further reproduction prohibited without permission.

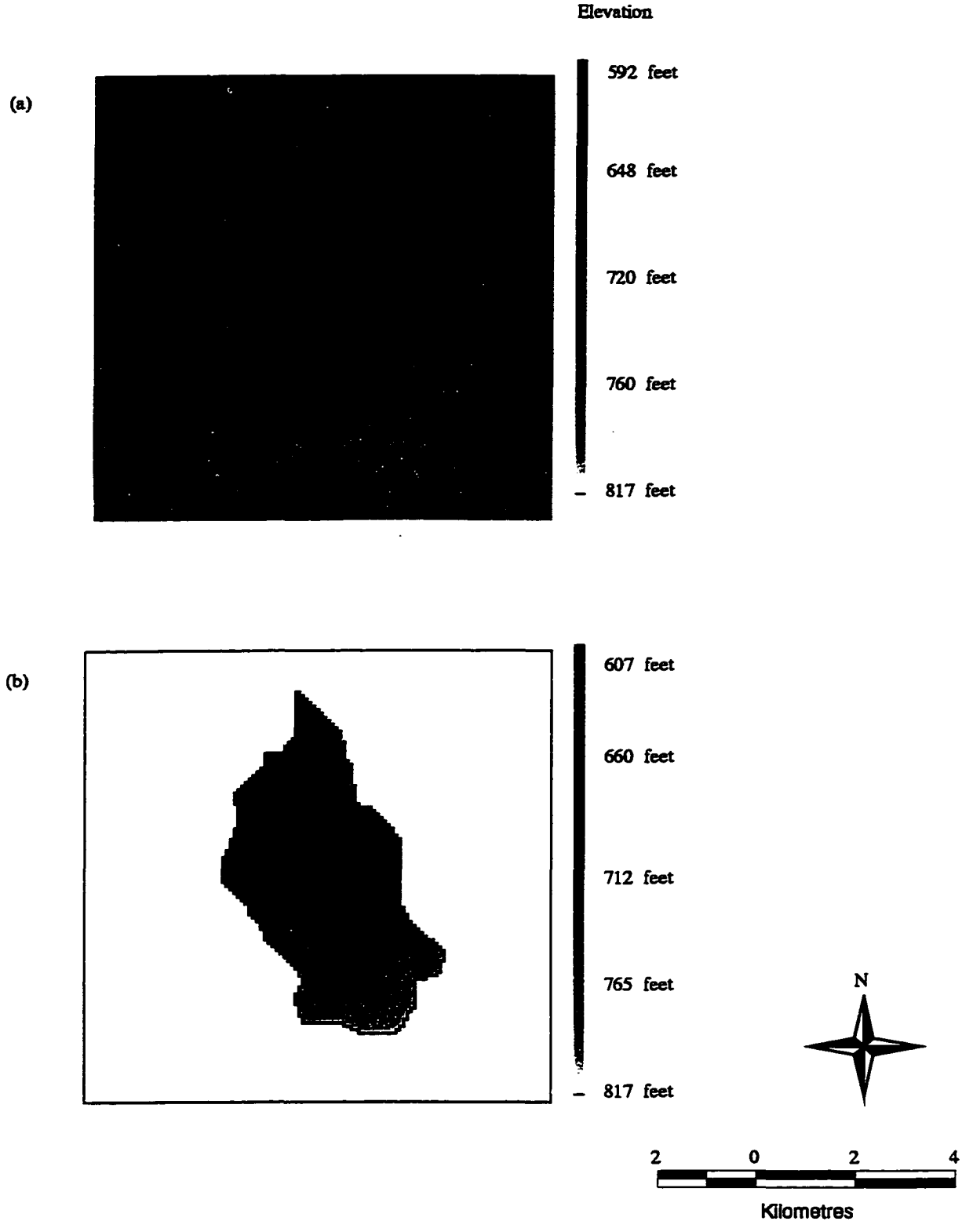

Figure 4.3. a) gray shaded DEM generated with TOPOGRID b) gray shaded DEM of watershed.

Reproduced with permission of the copyright owner. Further reproduction prohibited without permission.

NOTE TO USERS

Page(s) missing in number only; text follows. Page(s) were microfilmed as received.

UMI

Reproduced with permission of the copyright owner. Further reproduction prohibited without permission.

4.4 Watershed Mask Grid

The watershed mask is a binary raster map consisting of one's and zero's which identify the area falling inside (1) and outside of the watershed (0). The sequence of steps required to delineate the watershed boundary is shown in Figure 4.4.

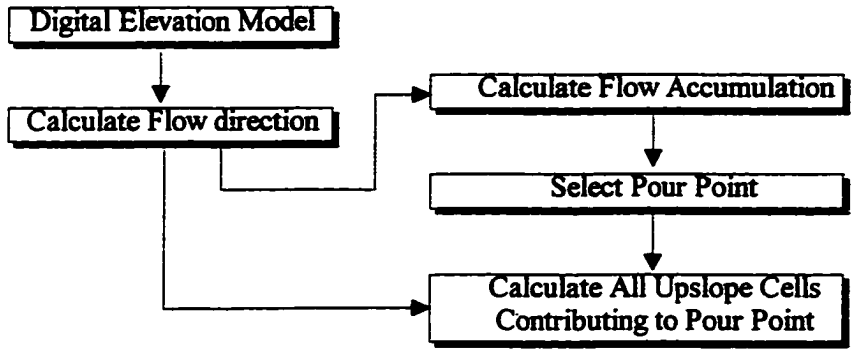

Figure 4.4. Flow chart of steps required to delineate watershed boundary.

A flow direction map was first derived from the DEM. The direction of flow from each cell (**x**) was based on the direction of steepest descent in relation to its eight surrounding cells (Figure 4.5). Cell **x** was assigned a numeric code of either 1,2,4,8,16,32,64 or 128 to indicate the direction of flow. For example, if the direction of steepest descent of cell **x** is directly downward, the cell would receive a flow direction code of 4.

32	64	128
16	**x**	1
8	4	2

Figure 4.5. Possible flow direction codes assigned to cell **x**.

Based on the flow direction map layer, a flow accumulation grid was produced which calculated all cells that flowed into each cell. From the flow accumulation grid, a general drainage network can be extracted by selecting cells that exceeded a specified

Reproduced with permission of the copyright owner. Further reproduction prohibited without permission.

value. High cell values indicate areas of concentrated flow. Following this, the location of the pour point of the watershed outlet can be determined. The stream network grid was essential when selecting the pour point. If the selected outlet is not located on a stream network cell, incorrect delineation would result. A pour point was selected at the mouth of the watersheds main river channel where it flowed into the Kulupielegu river. Finally, the watershed was delineated using the flow direction grid by calculating all cells which flowed into the selected pour point.

Results from the delineation showed some minor discrepancies between adjacent watersheds. Many of the major roads in this area were constructed through relatively flat dry areas where few stream crossings were required. Roads were elevated to prevent road washouts which created an artificial boundary between adjacent watersheds (Figure 4.6). The delineated watershed is shown with the two roads that should define a portion of the east and south edges of the watershed. In several sections it can be seen that the boundary either falls short of or extends beyond the road. This incorrect delineation is due to the resolution of the original contour elevation of 15.24 m which does not capture the slight changes in elevation. Streams and topography of the watershed are shown in Figure 4.7a and 4.7b.

The selected DEM elevation values were converted from feet to centimetres to maintain the DEM vertical resolution. A conversion factor (values were divided by 100) was then be applied in r.hydro.CASC2D to convert the elevation values from centimetres to meters. Using the standard export routine in ARC/INFO, the DEM was exported to GRASS. The grid coordinates were in feet due the TM projections system. Therefore, a conversion factor (values were divided by 3.281) was specified in r.hydro.CASC2D to convert the horizontal grid resolution from feet to metres.

The final delineated watershed consisted of 12,485 grid cells with a watershed area of 16.8 km^2.

Reproduced with permission of the copyright owner. Further reproduction prohibited without permission.

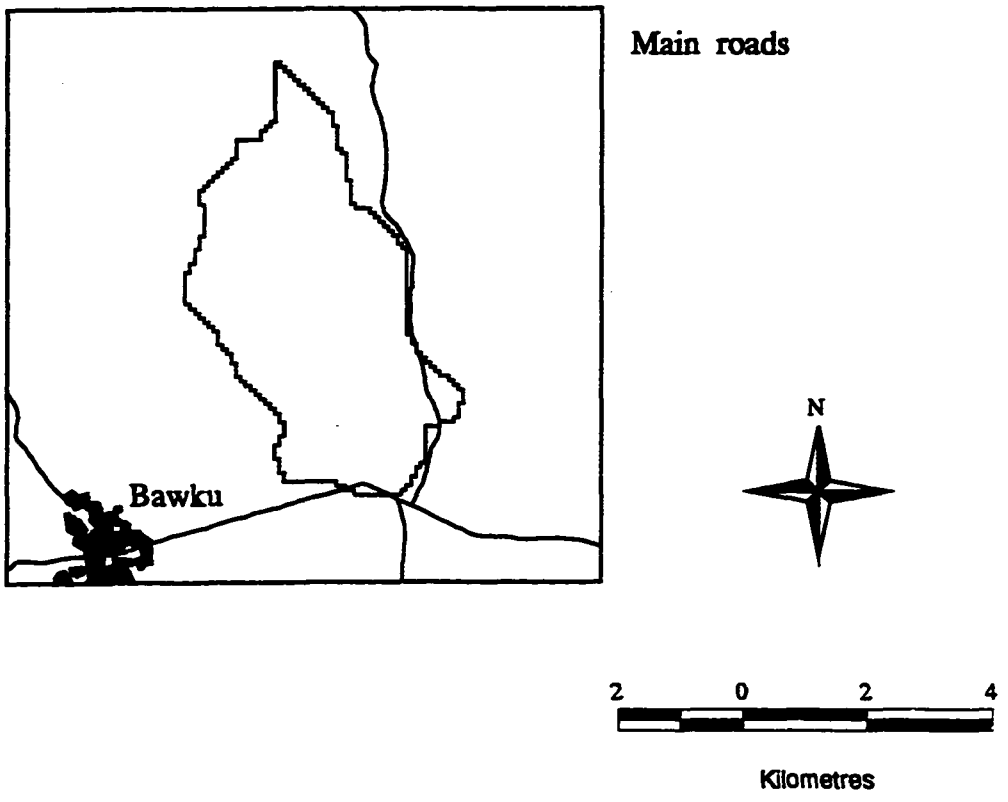

Figure 4.6. Main roads.

Reproduced with permission of the copyright owner. Further reproduction prohibited without permission.

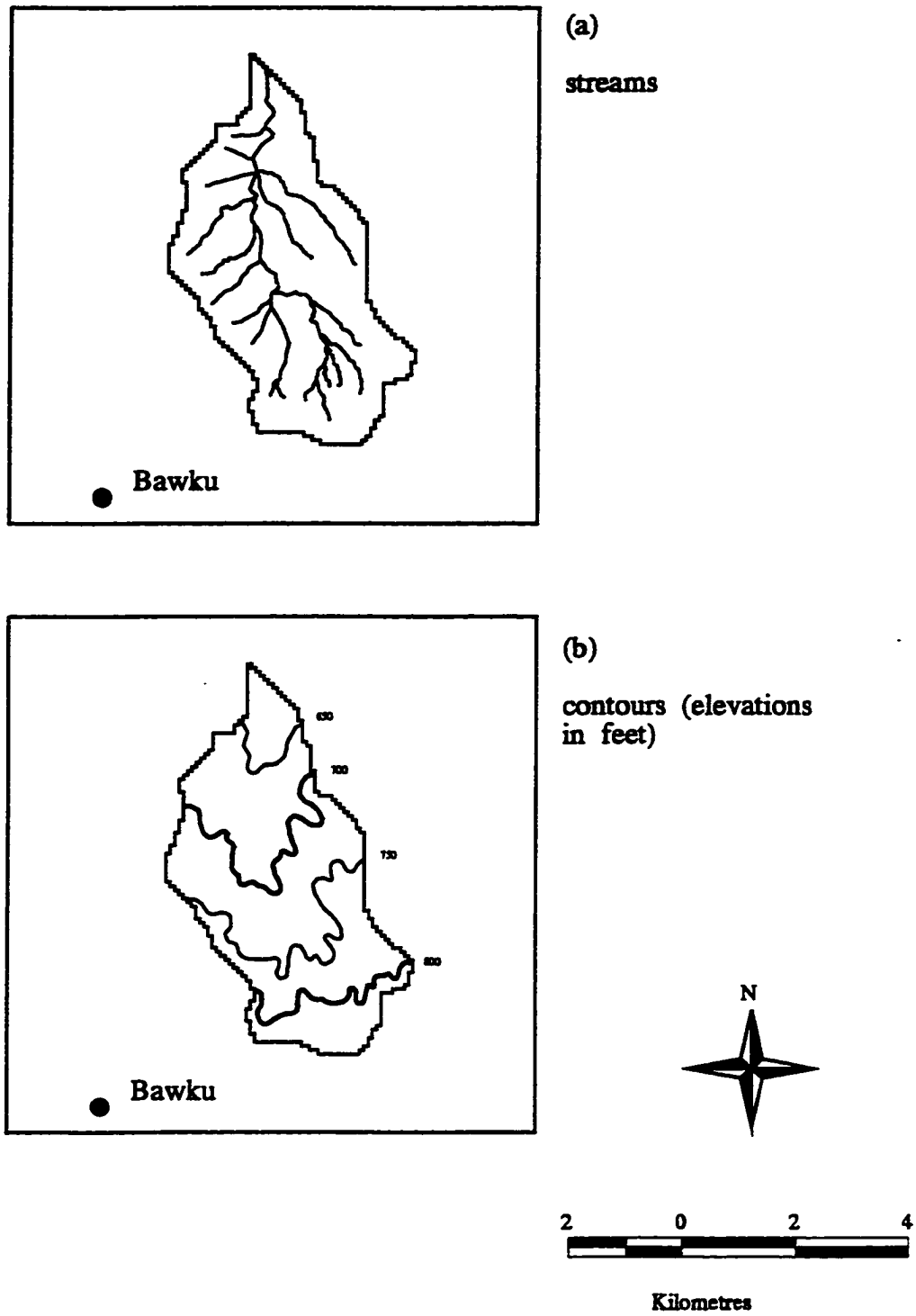

Figure 4.7. Watershed: a) streams and b) contours (elevations in feet).

Reproduced with permission of the copyright owner. Further reproduction prohibited without permission.

4.5 Infiltration Parameters Grid

Since detailed soils information was not available for the study area, soil information was obtained from a 1:250,000 scale soil quality map prepared by the Soil Research Institute of Ghana by Adu (1969). The soil quality map delineated arable and non-arable lands and provided a general description on soil texture, fertility, slope, erosion hazard and suitable agriculture activities for the area. Polygons representing the various soil qualities were digitized and attribute data was assigned to each polygon. In addition, stream data was digitized and stored as a separate coverage. Both coverages were then transformed to the Transverse Mercator projection system. The calculated RMS error was 28 m.

With the integration of data compiled from different sources and map scales, a problem often encountered was the misalignment of similar map features when overlaid. To ensure that the soils quality data was properly co-registered with the 1:50,000 scale maps, the 1:250,000 scale stream coverage was overlaid with the 1:50,000 scale stream coverage. By overlaying the stream coverages, the spatial accuracy of the two map sources was evaluated. The stream coverages were used since this feature was present on both 1:50,000 and 1:250,000 scale maps. The overlay revealed a systematic shift of approximately 300 m in the east-west (x-coordinate) direction between the two stream coverages. Although it was uncertain which maps contained the error, the Ghana Survey 1:50,000 scale map was considered to be correct for this study. The error was corrected by shifting the x-coordinates on the 1:250,000 scale coverage 300 m to the west. This resulted in a better match between the coverages. The same shift was also applied to the soil quality coverage. The corrected 1:250,000 streams coverage was not used in any further analysis.

The corrected soils coverage was converted to a 75 m grid and the watershed mask grid was used to mask the soils falling within the watershed. The masked soils grid consisted of three soil quality classifications (Figure 4.8a). A soil texture class was assigned to each soil quality class based on their drainage properties. The final soil grid consisted of two soil textures, clay and sandy loam (Figure 4.8b).

Reproduced with permission of the copyright owner. Further reproduction prohibited without permission.

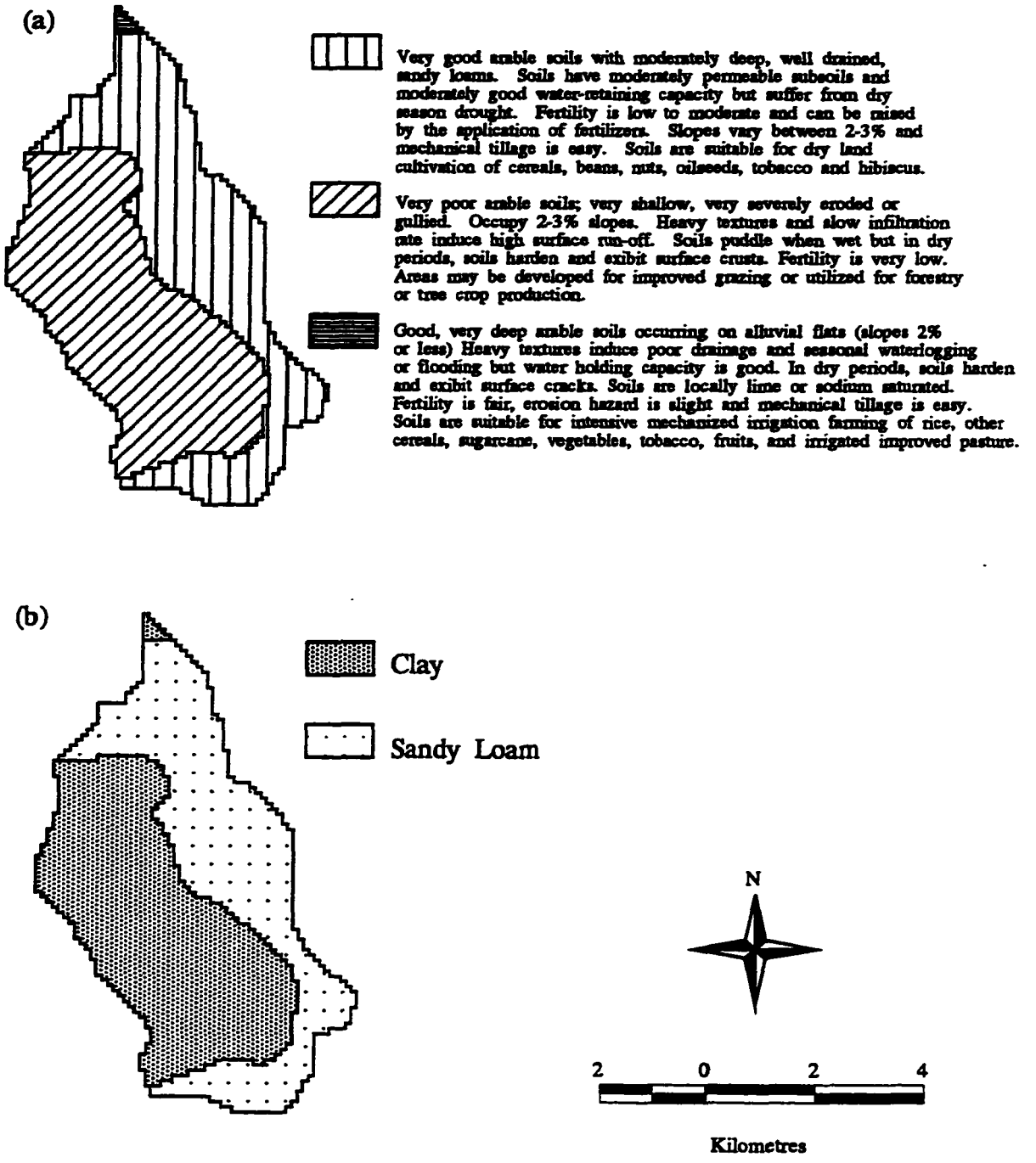

Figure 4.8. a) soil quality b) reclass of soil quality classes to soil texture based on drainage properties.

Reproduced with permission of the copyright owner. Further reproduction prohibited without permission.

Initial soil moisture is dependent on rainfall history and should be based on collected field data when available. Acheampong (1988) reports that between the months of August and September soils in northern Ghana are generally at field moisture capacity. Field moisture capacity defines the point where water within the soils larger pores (macropores) have been completely drained due to gravity and have been replaced with air. Since no soil field data was available, the initial soil moisture content for all soils were assumed to be equal to the soil water stored at the 1/3 bar atmosphere (field capacity) condition.

Four separate grids were created containing the required Green and Ampt infiltration parameters. Effective porosity (θ_e), wetting front capillary pressure (H_f), saturated hydraulic conductivity (K) and soil moisture at 1/3 bar (field capacity) values were estimated using the procedure outlined by Rawls *et al.* (1983b) and are summarized in Table 4.2 (see Appendix 3 for procedure). Each grid contained one infiltration parameter and varied according to the soil texture. The required fixed scale factor for each parameter was applied to each raster map and exported to GRASS.

Table 4.2. Estimated Green and Ampt soil infiltration parameters.

Soil Texture	Initial Moisture Content at 1/3 bar (volume)	Effective Porosity θ_e	Wetting Front Capillary Pressure H_f (cm)	Saturated Hydraulic Conductivity K (cm/hr)
Sandy Loam	0.18	0.45	11.00	3.0
Clay	0.38	0.40	100.00	0.01

4.6 Manning's n Value Grid

Landuse data was derived from SPOT multispectral (XS) satellite imagery acquired during the dry season in January 1991. Dry season data was selected due to the difficulty in acquiring cloud free data during the rainy season. The use of dry season

Reproduced with permission of the copyright owner. Further reproduction prohibited without permission.

data however, is advantageous because it increases the variability between major landuses, allowing for easier landuse identification. All image processing was carried out using ERDAS software. The image classification procedure consisted of two general steps: 1) image rectification; and 2) image classification.

4.6.1 Image Rectification

The process of projecting an image onto a flat plane that conforms to a specified map projection system is known as image rectification (ERDAS, 1991).

Image rectification involves locating ground control points (GCP) with known real world coordinate (reference) values from a map or image and their corresponding GCP locations (source) on an un-rectified image. Rectified coordinates are extrapolated from the GCP's with two polynomial equations (linear or non-linear) onto a rectified output image. The required transformation matrix of coefficients for each polynomial is calculated through least-squares regression analysis. The choice of a linear or non-linear polynomial is dependent on the complexity of the image being rectified. Images of hilly terrain typically have greater distortion requiring the use of non-linear polynomials. In comparison, less complex images, (*e.g.*, flat terrain), may only require a linear transformation.

The accuracy of the transformation is expressed as a Root Mean Square (RMS) error. Unlike the RMS error discussed earlier, this RMS error is calculated by re-transforming the map or image GCPs coordinates back to the un-rectified GCPs coordinate system. The distance between the un-rectified GCP and the re-transformed GCP is the RMS error, measured in the unit elements (pixels) of the image (ERDAS, 1991).

During the rectification process, pixel brightness values from the un-rectified image are assigned to pixels on an output image containing the rectified GCPs at a specified output pixel size. The un-rectified image GCPs are matched and overlaid onto the output image containing the rectified GCPs. Since the two grids are rarely aligned correctly, a resampling method is required to assign the un-rectified pixel values to the output image (ERDAS, 1991).

Reproduced with permission of the copyright owner. Further reproduction prohibited without permission.

Prior to image rectification, the general study area was subset from the full SPOT XS image. The SPOT subset covered approximately five Ghana Survey map sheets.

Seventy GCPs were initially located on both maps and SPOT XS image. Identifiable points included road intersections, stream intersections and dam impoundments. A linear transformation matrix and a RMS error was calculated using these points. Due to the relative flat terrain of the study area, a linear transformation was considered to be sufficient. The GCPs which contributed to the highest RMS error were removed and a new transformation matrix and RMS error was calculated. The above steps were repeated until the specified RMS error of 1 pixel or 20 m was reached. The final linear transformation matrix, using thirty nine GCPs, was used in the rectification process. Pixels were resampled to 25 m using a cubic convolution resampling method. The SPOT XS satellite image for the watershed is shown in Figure 4.9.

4.6.2 Landuse Classification

An unsupervised classification procedure was used to derive general landuse categories from the rectified satellite image. The first step involved submitting the image to a clustering algorithm that defined natural groupings or clusters within the image. The clustering algorithm relies on the assumption that brightness values representing a specific land covers are located closer together in spectral space, whereas, different land cover are separate. This assumption is also based on the fact that surface materials have different spectral reflectance in the visible and near-infrared bands. This can be illustrated by producing a simple 2 band scatterplot of brightness values which define their location in spectral space (Figure 4.10). Brightness values for water in the visible and near-infrared bands are typically very low. In contrast brightness values for vegetation are typically found to be much higher in the near-infrared band compared to the visible band.

Once the clusters have been defined, each pixel is examined and assigned to a class based on the criteria established by a decision rule, such as the Maximum Likelihood decision rule (ERDAS, 1991). Classes are identified and merged into meaningful categories.

Reproduced with permission of the copyright owner. Further reproduction prohibited without permission.

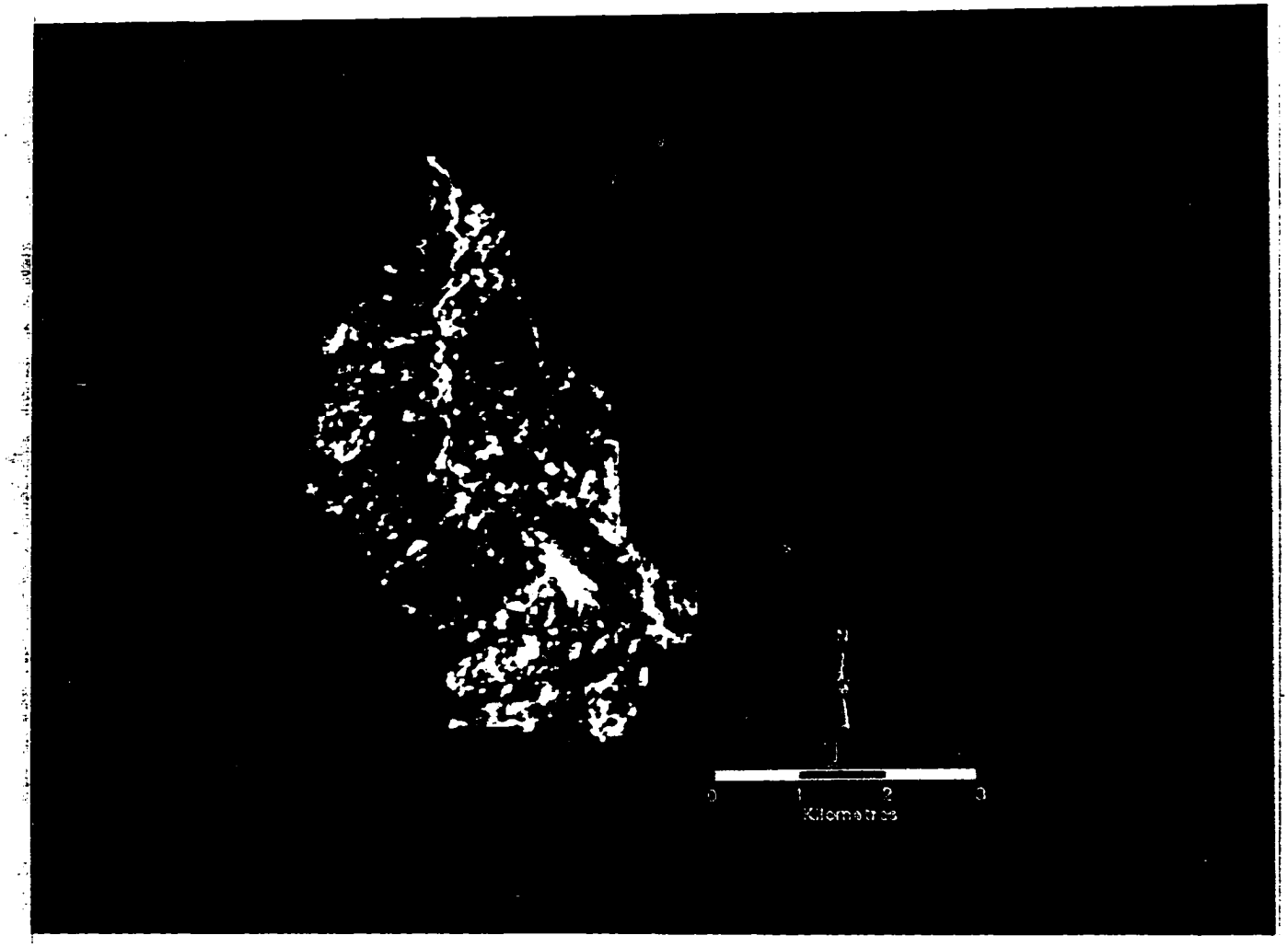

Figure 4.9. Dry season 1991 false color SPOT XS satellite image.

Reproduced with permission of the copyright owner. Further reproduction prohibited without permission.

Figure 4.10. Two band scatterplot in spectral space showing two possible clusters: water (•) and vegetation (o). Adapted from Lillesand and Kiefer (1994).

Two hundred and fifty-five clusters for this study were defined using the Iterative Self-Organising Data Analysis (ISODATA) technique and classified using a Maximum Likelihood decision rule.

The 255 classified groupings were re-classed into landuse classes. The landuse classes were based on available GPS (Global Positioning System) ground truth data collected in August 1994 around the Pusiga village, located approximately 10 km east of the study area (Runesson, pers. comm., 1996). The ground truth data fell within an area approximately 10 x 10 km in size. Ground truth data were collected along selected transects throughout sections of the 10 x 10 km area. Transects were selected that best captured the various landuse classes and was based on visual inspection of raw satellite data and field experience within the area.

While traversing a transect line, a Garmin GPS field unit was used to record the Longitude and Latitude transect location. Whenever a change in cultivation or vegetation occurred, the location was recorded and field notes were taken describing the general vegetation type and cultivation practices. In addition, roads and culverts were also mapped out with the GPS unit.

The GPS data was then differentially corrected using data collected at a temporary base station in Bawku. The data was then exported to ARC/INFO,

Reproduced with permission of the copyright owner. Further reproduction prohibited without permission.

transformed to the Transverse Mercator system and then exported as a vector file (DIG file) to ERDAS.

This data was used in lieu of no available ground truth data within the study area and was assumed to be acceptable since landuse within this area is similar to conditions occurring within the watershed under study.

Once in an ERDAS vector file format, the transect lines and roads were overlaid onto the classified image to verify proper registration. It was at this stage that the GPS data was found to be systematically shifted approximately 100 m north of the features on the satellite image. Since the SPOT image was rectified to the 1:50,000 Ghana survey maps from which all other data was based, the satellite image coordinates were assumed to be correct. The error was corrected by applying a positive systematic shift of 100 m to all the y-coordinates of the GPS data .

Based on the GPS transects, field notes and using photo interpretation skills, the 255 classes were classified into four landuse classes (Table 4.3.).

Table 4.3. Landuse class codes and description.

Landuse Class	Class Description
1	Non-Agriculture: dense brush
2	Non-Agriculture: brushland / range with short grasses and low brush
3	Agriculture: corn and millet with some short grasses.
4	Agriculture: groundnuts and beans, and bare soil

To match the DEM grid cell size of 75 m, the landuse map was resampled from 25 m to 75 m using a 3x3 majority rule filter. The filter merged the 9 cells falling within the 3x3 filter and assigned a value to the new cell based on the majority landuse class. The landuse map was exported to ARC/INFO as a grid and reclassified to Manning's n values based on published values and general knowledge of the area (see Table A.1.2 in

Reproduced with permission of the copyright owner. Further reproduction prohibited without permission.

Appendix 1). Since the Manning's n values are expressed as floating point values and all grid values must be in a non-decimal format, a scaling factor was applied by multiplying all values with 1000. Thus, a scaled value of 400 would represent a Manning's n value of 0.40. The watershed boundary grid was used to mask the final landuse grid as shown in Figure 4.11. Manning's n values assigned to each landuse class and an area summary of each class is listed in Table 4.4. The final landuse map was exported to GRASS.

Table 4.4. Summary of assigned Manning's n values and percentage of area for each landuse class.

Landuse Class Code	Assigned Manning's n value	Area of watershed (%)
1	0.40	3
2	0.15	8
3	0.10	35
4	0.05	54

4.7 Rainfall Event

Currently, only daily rainfall data are collected at the Bawku meteorological monitoring station, the nearest station to the study area. This data unfortunately does not provide any information on rainfall duration or rainfall intensity. Therefore, a hypothetical uniform rainfall event of 1 hour with a rainfall intensity of 30 mm/hr was selected as the rainfall event for this study.

Reproduced with permission of the copyright owner. Further reproduction prohibited without permission.

Figure 4.11. Landuse classes derived from dry season SPOT XS satellite image.

Reproduced with permission of the copyright owner. Further reproduction prohibited without permission.

4.8 Watershed Outlet Location and Slope and Computational Time Step

The location of the watershed outlet was located by:

1) displaying the flow accumulation grid in ARC/INFO;
2) selecting the cell location at the watershed outlet; and
3) recording the displayed x and y cell location.

The outlet slope was calculated as the elevation difference from the next upstream cell flowing in the x-direction and the outlet cell divided by the cell size. The calculated outlet slope was 0.004 (*i.e.*, 0.4%). A computational time step of 10 seconds was fixed for all landuse scenario simulations.

Reproduced with permission of the copyright owner. Further reproduction prohibited without permission.

CHAPTER 5: PARAMETER SENSITIVITY ANALYSIS

5.1 Purpose

A sensitivity analysis was performed to test selected model input parameters for the greatest influence on the watershed hydrological response. Watershed parameters investigated included: 1) grid cell size; 2) soil infiltration parameters based on soil texture; 3) initial soil moisture at 1/3 bar (field capacity); and 4) soil moisture at 15 bar (wilting point).

Due to the large number of possible parameter combinations and the difficulty in interpolating them, uniform parameter values were investigated instead of spatially varying parameters. In addition, due to difficulties in implementing the channel routing option, no channel routing was performed, Therefore, all surface flow was routed as overland flow.

A spatial and temporally uniform rain event of 1 hour with a 30 mm/hr rainfall intensity was run for a total rainfall-runoff event time of 24 hrs.

5.2 Sensitivity Analysis for Grid Cell Size

To test the model sensitivity to various grid cell sizes, two more DEM and watershed masks were generated at 100 m and 200 m grid cell sizes following the procedure outlined in section 4.3 and 4.4.

To check for potential errors in the DEM, a rainfall event was first simulated for each grid cell size using a spatially uniform Manning's n value of 0.05 without soil infiltration. A computational time step of 30 seconds was used for the 100 m and 200 m grid cell size and a 10 second time step for the 75 m grid cell size. A lower time step for the 75 m grid cell size was required to maintain numerical stability. The watershed outlet location was determined and the bed slope recalculated as 0.002 and 0.007 for the

Reproduced with permission of the copyright owner. Further reproduction prohibited without permission.

100 m and 200 m DEM, respectively. Infiltration was neglected in an effort to separate the effect of infiltration from grid cell size on the watersheds hydrologic response (Table 5.1).

Table 5.1 Summary of r.hydro.CASC2D input parameters required for grid cell sensitivity simulations

	Grid cell size		
Input	75 m	100 m	200 m
watershed_mask[1]	basin_75	basin_100	basin_200
elevation[1]	dtm75	dtm100	dtm200
outlet			
x-coordinate	1,180,455	1,180,483	1,181,154
y-coordinate	2,344,838	2,344,731	2,344,241
slope	0.004	0.002	0.007
Manning_n	0.05	0.05	0.05
unif_rain_int	30	30	30
time_step	10	30	30
rain_duration	3,600	3,600	3,600
tot_time	86,000	86,000	86,000
unit_el_conv	100	100	100
unit_space	3.281	3.281	3.281
write_time_step	1200	1200	1200

[1] Raster map

During each simulation, surface water depth maps were generated at twenty minute intervals and examined for areas containing unrealistic amounts of surface water accumulation. Examination of the surface water depth maps revealed that all three DEM contained several internal sinks. These internal sinks are a result of flow directions

Reproduced with permission of the copyright owner. Further reproduction prohibited without permission.

between adjacent grid cells being restricted to the horizontal and vertical directions in r.hydro.CASC2D. Each DEM was manually edited by adjusting the elevation values to ensure drainage would flow to an adjacent grid cell in either the horizontal or vertical flow direction. The above simulation procedure was repeated to ensure all sinks were corrected.

Comparisons were made between the three grid cell sizes and assessed for the number of grid cells, total area, length of perimeter and average slope. Watershed area, perimeter and average slope were similar (Figure 5.1). However, with regards to the spatial extent of the watershed, a noticeable error can been seen with the 200 m grid cell size where portions of several streams extended beyond the border of the watershed. In addition, due to the low relief surrounding the watershed outlet, a portion of the main channel ran along the edge of the watershed boundary. There was a large difference between the number of cells required to represent the watershed, with the number of cells decreasing as cell size increased.

Results of the models sensitivity to grid size is shown in the form of an outlet hydrograph in Figure 5.2. As grid cell size decreased, it can be seen that a substantial increase in peak discharge occurred. Only a minimal change in time to peak occurred with a total difference of 30 minutes between the 75 m and 200 m grid cell size. Since no infiltration was computed, all rainfall appeared as surface runoff.

Reproduced with permission of the copyright owner. Further reproduction prohibited without permission.

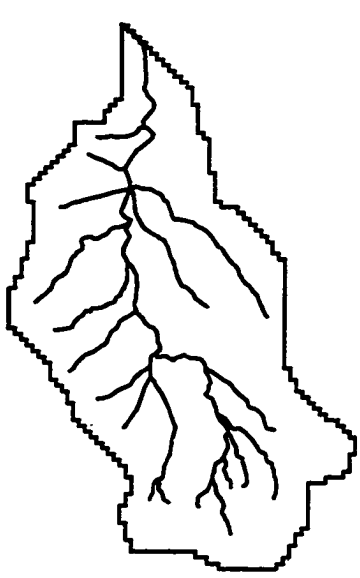

Grid cell size: 75 m

Number of Cells: 2,485
Watershed Area (square km): 16.8
Watershed Perimeter (m): 23,500
Average Slope (%): 1.4

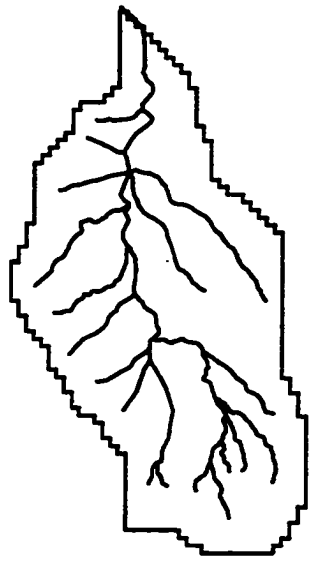

Grid cell size: 100 m

Number of Cells: 1,621
Watershed Area (square km): 16.2
Watershed Perimeter (m): 21,800
Average Slope (%): 1.4

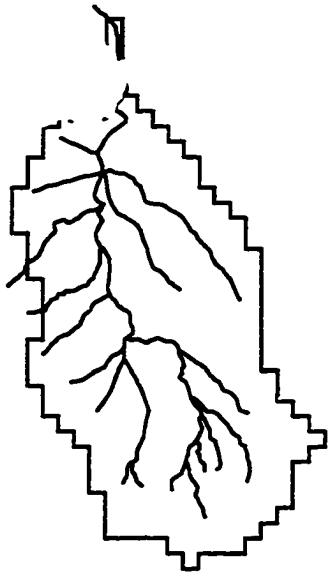

Grid cell size: 200 m

Number of Cells: 388
Watershed Area (square km): 16.5
Watershed Perimeter (m): 22,800
Average Slope (%): 1.3

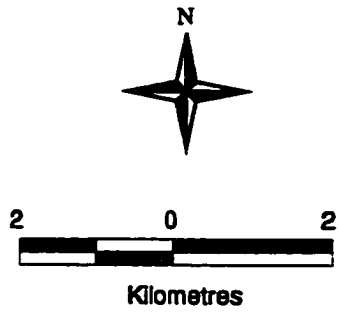

Figure 5.1. Summary of changes to watershed area, watershed perimeter, average slope, number of cells and spatial extent for three different cell sizes: 75 m, 100 m and 200 m.

Reproduced with permission of the copyright owner. Further reproduction prohibited without permission.

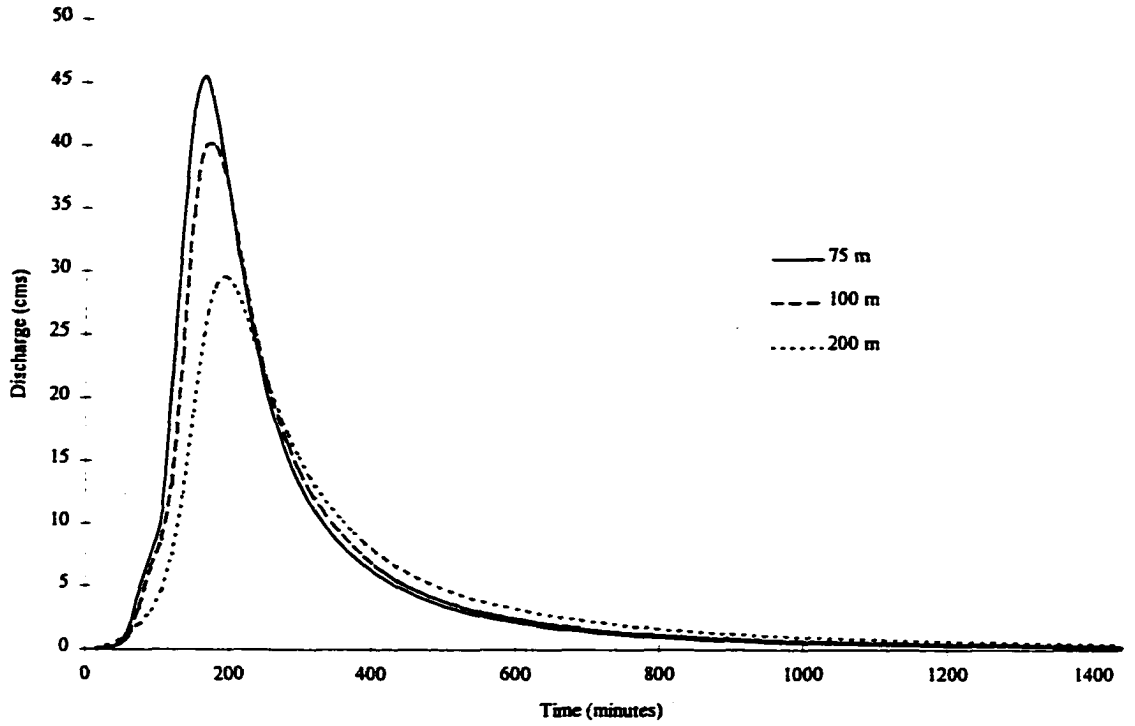

Figure 5.2. Hydrographs illustrating sensitivity to 75 m, 100 m and 200 m grid cell sizes.

5.3 Sensitivity Analysis for Green and Ampt Infiltration Parameter

In an effort to simplify the possible combinations of the Green and Ampt soil infiltration parameters, infiltration parameters were not examined individually but were assessed according to their values based on soil texture using values from Rawls *et al.* (1983b). In addition, initial soil moisture at 1/3 bar and 15 bar tension were examined for each soil texture. A uniform Manning's n value of 0.05 was used for all simulations. Model inputs for the Green and Ampt infiltration sensitivity analysis are summarized in Table 5.2.

For each soil texture, the required Green and Ampt soil infiltration parameter grid maps were prepared following the same procedure outlined in section 4.5 with the exception that spatially uniform values were used for the whole watershed (Table 5.3).

Results of the soil infiltration parameters sensitivity analysis are summarized in Table 5.4. Hydrographs for soils that contributed the three highest runoff volumes are shown in Figure 5.3.

Reproduced with permission of the copyright owner. Further reproduction prohibited without permission.

Table 5.2. Summary of r.hydro.CASC2D input parameters required for Green and Ampt soil infiltration sensitivity simulations.

Input	Soil Texture				
	Clay	Silty Clay	Sandy Clay	Silty Clay Loam	Clay Loam
watershed_mask[1]	mask_75	mask_75	mask_75	mask_75	mask_75
elevation[1]	dtm75	dtm75	dtm75	dtm75	dtm75
outlet					
x-coordinate	1,180,455	1,180,455	1,180,455	1,180,455	1,180,455
y-coordinate	2,344,838	2,344,838	2,344,838	2,344,838	2,344,838
slope	0.004	0.004	0.004	0.004	0.004
conductivity[1]	cond	cond	cond	cond	cond
capillary[1]	cap	cap	cap	cap	cap
porosity[1]	pore	pore	pore	pore	pore
moisture[1]	moist	moist	moist	moist	moist
Manning_n	0.05	0.05	0.05	0.05	0.05
unif_rain_int	30	30	30	30	30
time_step	10	10	10	10	10
rain_duration	3,600	3,600	3,600	3,600	3,600
tot_time	86,000	86,000	86,000	86,000	86,000
unit_el_conv	100	100	100	100	100
unit_space	3.281	3.281	3.281	3.281	3.281

[1] Raster map

Reproduced with permission of the copyright owner. Further reproduction prohibited without permission.

Table 5.2. (continued) Summary of r.hydro.CASC2D input parameters required for Green and Ampt soil infiltration sensitivity simulations.

Input	Soil texture				
	Sandy Clay Loam	Silt Loam	Loam	Sandy loam	Loamy Sand
watershed_mask[1]	mask_75	mask_75	mask_75	mask_75	mask_75
elevation[1]	dtm75	dtm75	dtm75	dtm75	dtm75
outlet					
x-coordinate	1,180,455	1,180,455	1,180,455	1,180,455	1,180,455
y-coordinate	2,344,838	2,344,838	2,344,838	2,344,838	2,344,838
slope	0.004	0.004	0.004	0.004	0.004
conductivity[1]	cond	cond	cond	cond	cond
capillary[1]	cap	cap	cap	cap	cap
porosity[1]	pore	pore	pore	pore	pore
moisture[1]	moist	moist	moist	moist	moist
Manning_n	0.05	0.05	0.05	0.05	0.05
unif_rain_int	30	30	30	30	30
time_step	10	10	10	10	10
rain_duration	3,600	3,600	3,600	3,600	3,600
tot_time	86,000	86,000	86,000	86,000	86,000
unit_el_conv	100	100	100	100	100
unit_space	3.281	3.281	3.281	3.281	3.281

[1] Raster map

Reproduced with permission of the copyright owner. Further reproduction prohibited without permission.

Table 5.3. Estimated Green and Ampt soil infiltration parameters based on soil texture.

Soil Texture	Initial Moisture Content at 1/3 bar (volume)	Initial Moisture Content at 15 bar (volume)	Effective Porosity θ_e	Wetting Front Capillary Pressure H_f (cm)	Saturated Hydraulic Conductivity K (cm/hr)
Loamy Sand	0.125	0.060	0.375	6.00	10.00
Sandy Loam	0.18	0.070	0.45	11.0	3.00
Loam	0.25	0.120	0.40	20.0	0.80
Silt Loam	0.275	0.125	0.475	29.0	0.60
Sandy Clay Loam	0.25	0.16	0.32	10.0	1.00
Clay Loam	0.35	0.20	0.36	35.0	0.15
Silty Clay Loam	0.37	0.28	0.40	60.0	0.06
Sandy Clay	0.325	0.225	0.325	28.0	0.18
Silty Clay	0.425	0.275	0.475	100.0	0.07
Clay	0.38	0.28	0.40	100.0	0.01

Reproduced with permission of the copyright owner. Further reproduction prohibited without permission.

Table 5.4. Summary of model sensitivity to soil infiltration using various Green and Ampt parameters based on soil texture and initial soil moisture at 1/3 and 15 bar. Volume outflow and volume infiltrated represent the percentage of total rainfall volume.

Time	Initial Soil Moisture at 1/3 bar				Initial soil moisture at 15 bar			
	Time to peak (min)	Peak discharge (cms)	Volume outflow (%)	Volume infiltrated (%)	Time to peak (min)	Peak discharge (cms)	Volume outflow (%)	Volume infiltrated (%)
Loamy Sand	n/a	0.00	0.0	100	n/a	0.00	0.0	100
Sandy Loam	n/a	0.00	0.0	100	n/a	0.00	0.0	100
Loam	n/a	0.00	0.0	100	n/a	0.00	0.0	100
Silt Loam	n/a	0.00	0.0	100	n/a	0.00	0.0	100
Sandy Clay Loam	148	0.11	0.1	100	n/a	0.00	0.0	100
Clay Loam	n/a	0.00	0.0	100	n/a	0.00	0.0	100
Silty Clay Loam	n/a	0.00	0.0	100	n/a	0.00	0.0	100
Sandy Clay	167	38.48	73.0	27	208	14.00	29.0	71
Silty Clay	194	20.50	42.0	58	279	3.37	9.0	91
Clay	168	39.43	80.0	18	179	31.16	63.5	36.5

Reproduced with permission of the copyright owner. Further reproduction prohibited without permission.

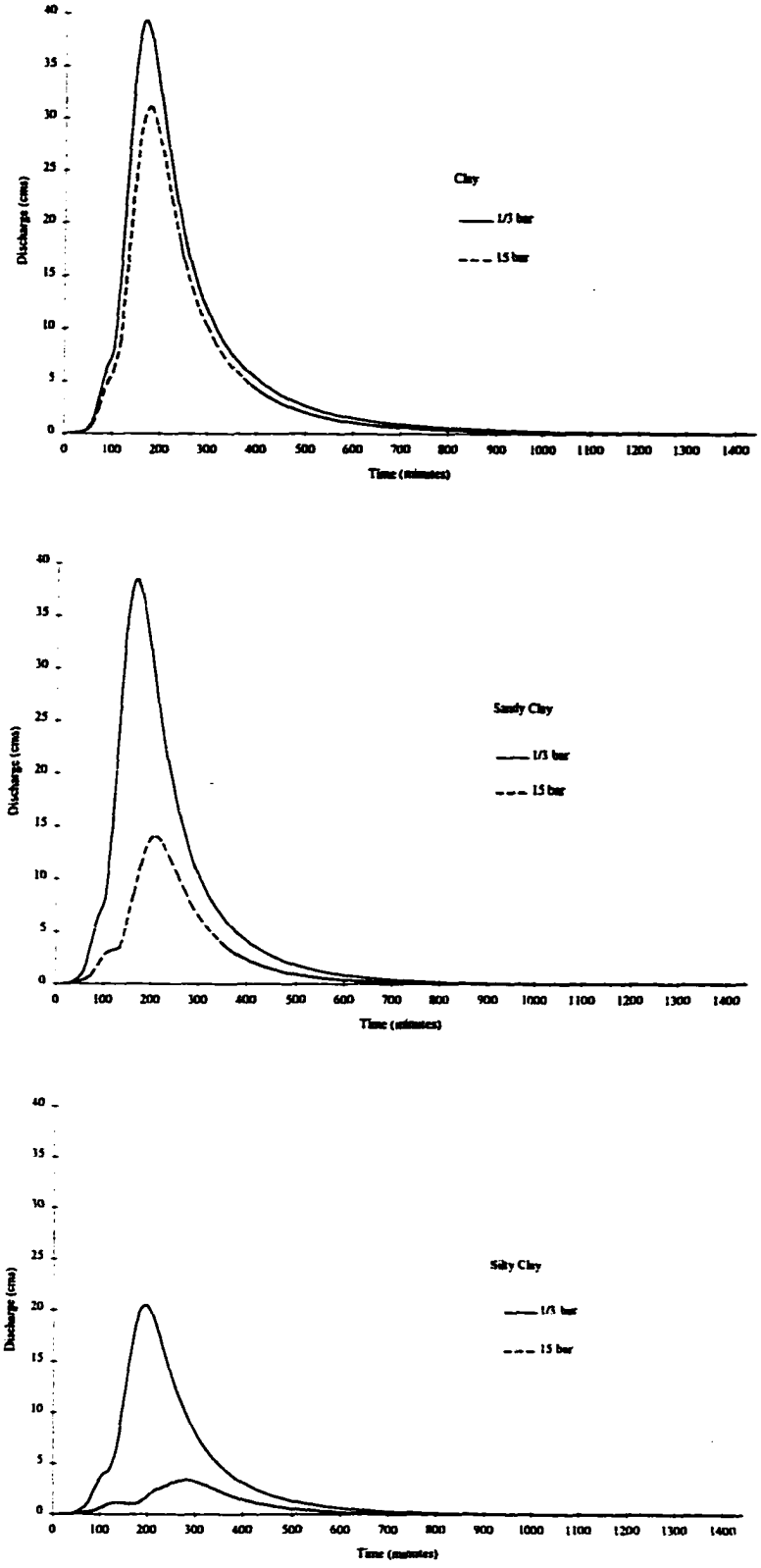

Figure 5.3. Hydrographs illustrating sensitivity to Green and Ampt soil infiltration parameters based on soil texture and initial soil moisture at 1/3 bar and 15 bar.

Reproduced with permission of the copyright owner. Further reproduction prohibited without permission.

Only three soil textures, clay, silty clay and sandy clay produced any substantial runoff with the remaining soil textures producing no runoff due to complete or near complete infiltration under a 1 hr, 30 mm/hr uniform rainfall event (Table 5.4). Comparisons between initial soil moisture showed no difference with the coarser textured soils. With reference to the hydrographs in Figure 5.3, a large effect on peak discharge was shown with regards to changes in initial moisture content between 1/3 bar and 15 bar for clay, silty clay and sandy clay with peak discharges decreasing with the finer texture soils.

5.4 Sensitivity Analysis for Manning's n Overland Roughness Coefficient

Four Manning's n overland roughness coefficient values were selected for analysis. Values were selected that reflected current conditions found within the watershed. Values tested were 0.05, 0.10, 0.15 and 0.40. All simulations were performed using spatially uniform Manning's n values with no infiltration. Again, infiltration was neglected in order to separate the effects of infiltration from changes in Manning's n values with respect to the watersheds hydrologic response. Model inputs for the Manning's n value sensitivity analysis are summarized in Table 5.5. Results are shown in Figure 5.4.

Changes in Manning's n values have a large effect on peak discharge and time to peak. As values increased, peak discharge decreased and time to peak was further delayed. A reduction in the Manning's value reduced surface friction and enabled surface runoff to reach the outlet faster, so the hydrographs rise and recession is rapid. An increase in Manning's value from 0.05 to 0.10, for example, resulted in a 48% decrease in peak discharge with a 123 minutes difference in peak times.

Reproduced with permission of the copyright owner. Further reproduction prohibited without permission.

Table 5.5. Summary of r.hydro.CASC2D input parameters required for Manning's n sensitivity simulations.

Input	Manning's n 0.05	0.10	0.15	0.40
watershed_mask[1]	mask_75	mask_75	mask_75	mask_75
elevation[1]	dtm75	dtm75	dtm75	dtm75
outlet				
x-coordinate	1,180,455	1,180,455	1,180,455	1,180,455
y-coordinate	2,344,838	2,344,838	2,344,838	2,344,838
slope	0.004	0.004	0.004	0.004
Manning_n	0.05	0.05	0.05	0.05
unif_rain_int	30	30	30	30
time_step	10	30	30	30
rain_duration	3,600	3,600	3,600	3,600
tot_time	86,000	86,000	86,000	86,000
unit_el_conv	100	100	100	100
unit_space	3.281	3.281	3.281	3.281

[1] Raster map

Reproduced with permission of the copyright owner. Further reproduction prohibited without permission.

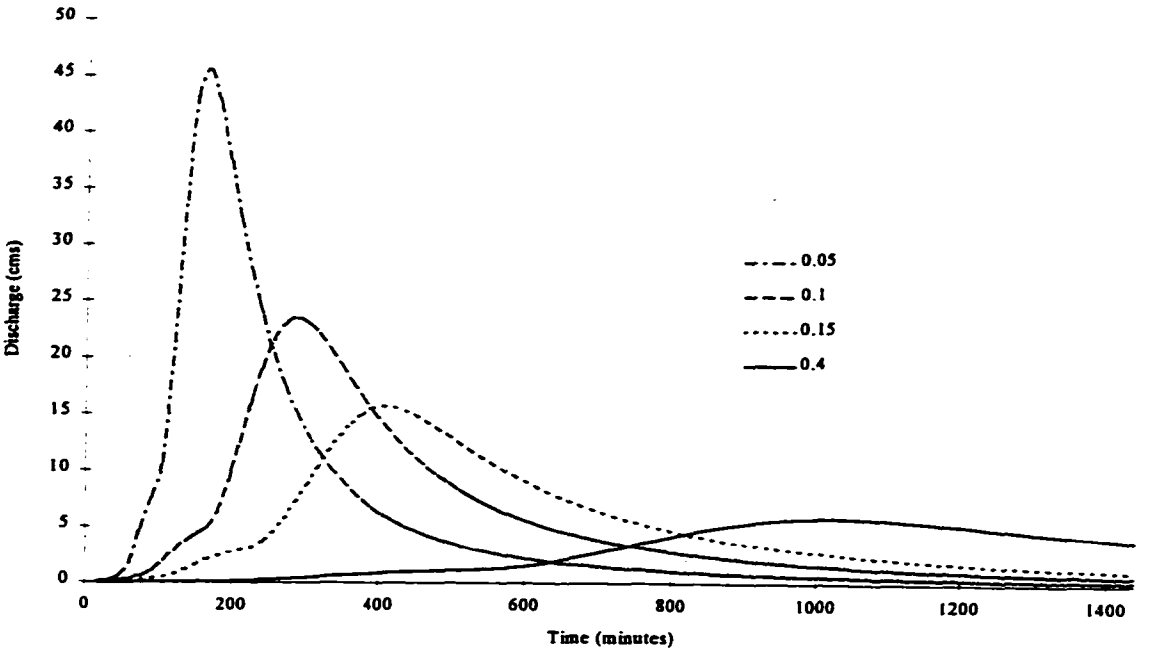

Figure 5.4. Hydrographs illustrating sensitivity of Manning's n overland flow parameter.

Reproduced with permission of the copyright owner. Further reproduction prohibited without permission.

CHAPTER 6: LANDUSE SCENARIOS

6.1 Purpose

To demonstrate the application of r.hydro.CASC2D and its use in evaluating the hydrologic response to changes in landuse practices, two hypothetical future landuse scenarios were simulated and evaluated for changes in surface runoff and infiltration volume, peak discharge and time to peak discharge at the watershed outlet. Results were evaluated to determine if proposed landuse practices effectively reduced runoff. The selected scenarios were based on situations which were believed to be realistically achievable within the watershed with some effort from landuse planners and land owners.

For evaluation purposes a baseline was required for comparisons with proposed landuse scenarios. A baseline was selected based on landuse derived from a classified 1991 SPOT XS satellite imagery as described in Chapter 4. Two hypothetical future landuse scenarios were developed from the baseline landuse map which are reflected within the model as a change in the Manning's n values. It can be expected that a change of landuse may alter other input parameters, such as soil hydraulic properties. However, for this study, only changes to Manning's n values were adjusted while all other input parameters remained fixed. In addition, changes were concentrated within specific contiguous regions since rehabilitation efforts would normally be implemented within specific areas and not randomly distributed throughout the watershed.

6.2 Landuse Scenarios

Crops, such as, groundnuts and beans provide sparse vegetative cover and leave little crop residue after harvest. Collection of remaining crop residue for fodder and fuel, and grazing of animals on plant stalks during the dry season removes any remaining ground cover. These bare areas experience excessive runoff at the start

Reproduced with permission of the copyright owner. Further reproduction prohibited without permission.

of the rainy season. Soil losses ranging from 2.2 tonnes ha^{-1} yr^{-1} for bare soils and 0.1 tonnes ha^{-1} yr^{-1} for grass and legumes mixtures have been reported from experimental runoff plots at Manga (Dept. of Geography, 1992). Landuse scenarios selected were directed towards area rehabilitation by increasing vegetation cover in an effort to reduce soil erosion by reducing the erosive effects of surface runoff.

The first landuse scenario, Case 1, was selected to investigate the impact of shifting agriculture production from groundnuts and beans to maize and millet crops, which provide increased ground cover. The second landuse scenario selected, Case 2, was directed towards investigating the impact of converting areas identified as poor arable and severely eroded soils under groundnut and bean agriculture to range land and crop tree production. The three landuse scenarios are summarized as follows:

Baseline: Landuse conditions as classified from 1991 SPOT XS satellite imagery.

Case 1: Change of agriculture from groundnuts and beans to maize and millet agriculture.

Case 2: Conversion of beans and groundnuts agriculture to range land and crop tree production on poor arable soils.

For Case 1, a 2.4 km^2, contiguous area under groundnuts and beans production was selected in the southern portion of the watershed and reclassed to maize and millet agriculture (Figure 6.1). For Case 2, all agriculture areas under groundnut and bean production on poor arable soils was identified and reclassed to range land (Figure 6.2). Manning's n values were then assigned to both new landuse grids as outlined in section 4.6 and exported to GRASS. The percentage of area for each landuse and its associated change for each landuse scenario is summarized in Table 6.1.

Reproduced with permission of the copyright owner. Further reproduction prohibited without permission.

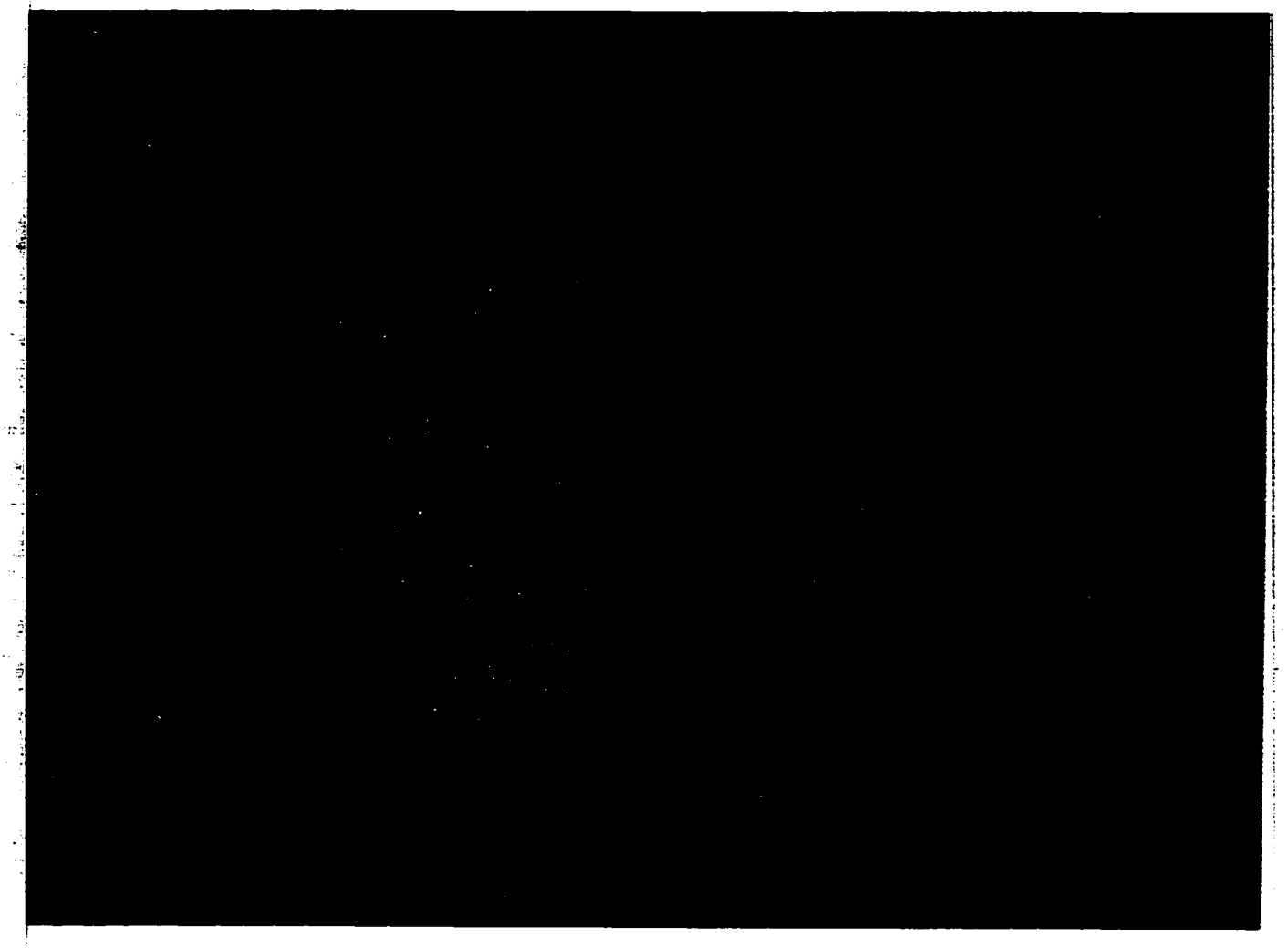

Figure 6.1. Landuse class distribution for Case 1.

Reproduced with permission of the copyright owner. Further reproduction prohibited without permission.

Figure 6.2. Landuse class distribution for Case 2.

Reproduced with permission of the copyright owner. Further reproduction prohibited without permission.

Table 6.1. Percentage of watershed area of each landuse class and its associated change for each landuse scenario (shown in brackets).

Landuse	Baseline	Case 1	Case 2
Non-Agriculture: dense brush	3	3 (0)	3 (0)
Non-Agriculture: brushland / range with short grasses and some low brush	8	8 (0)	35 (-27)
Agriculture: corn and millet, some short grasses.	35	52(+17)	35 (0)
Agriculture: groundnuts and beans, with bare soil.	54	37 (-17)	27 (-27)

Simulation events were run using the prepared data files described in Chapter 4 and the appropriate Manning's n value grid. A one hour rainfall event with a uniform rainfall intensity of 30 mm/hr for a total rainfall-runoff simulation event time of 15 hours was used for all three simulations. A 10 second computational time step was also used for all three simulations. No channel routing was performed. All surface runoff was routed as overland flow and channels were assumed wide (equal to cell size) with infiltration occurring within the stream channels. Model inputs required for the landuse scenarios are summarized in Table 6.2. Landuse scenario simulation results are graphically shown in Figure 6.1 and summarized in Table 6.3.

Reproduced with permission of the copyright owner. Further reproduction prohibited without permission.

Table 6.2. Summary of r.hydro.CASC2D input parameters required for landuse scenarios.

	Landuse scenarios		
Input	Baseline	Case 1	Case 2
watershed_mask[1]	mask_75	mask_75	mask_75
elevation[1]	dtm75	dtm75	dtm75
outlet			
x-coordinate	1,180,455	1,180,455	1,180,455
y-coordinate	2,344,838	2,344,838	2,344,838
slope	0.004	0.004	0.004
conductivity[1]	cond	cond	cond
capillary[1]	cap	cap	cap
porosity[1]	pore	pore	pore
moisture[1]	moist	moist	moist
roughness_map[1]	baseline	case1	case2
unif_rain_int	30	30	30
time_step	10	10	10
rain_duration	3,600	3,600	3,600
tot_time	86,000	86,000	86,000
unit_el_conv	100	100	100
unit_space	3.281	3.281	3.281

[1] Raster map

Reproduced with permission of the copyright owner. Further reproduction prohibited without permission.

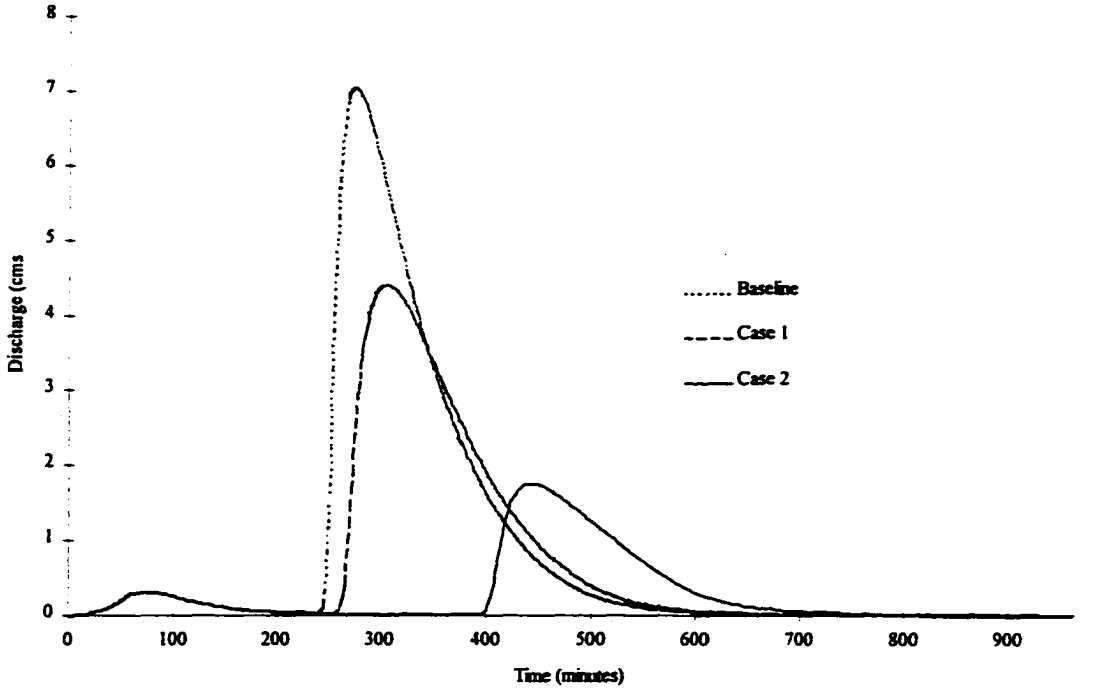

Figure 6.3. Hydrographs illustrating effect of different landuse scenarios.

Table 6.3. Summary results of landuse scenarios. Volume outflow and volume infiltrated represents the percentage of total rainfall volume.

Landuse Scenario	Time to peak (min)	Peak discharge (cms)	Volume outflow (%)	Volume infiltrated (%)
Baseline	275	7.04	9.30	90
Case 1	306	4.41	7.11	92
Case 2	444	1.76	3.18	96

Reproduced with permission of the copyright owner. Further reproduction prohibited without permission.

As shown in Figure 6.3, a minor peak occurs at the beginning of the storm for all three landuse scenarios which results from surface runoff due to the low infiltrating clay soils adjacent to the watershed outlet. The minor peak is identical for all three simulations since no landuse changes occurred in this portion of the watershed. Similar to the first peak, the second peak comes from surface runoff from the low infiltrating clay soils found within the south west portion the watershed. Since no runoff occurs on the sandy loam soils, a time delay occurs until surface runoff from the low infiltrating areas reach the watershed outlet. Because all surface runoff is being routed as overland flow, re-infiltration from surface runoff from the low infiltrating soils occurs when runoff reaches the high infiltrating sandy loam soils. Since the DEM was constructed with stream data, overland flow concentrates along stream flow paths as it moves towards the watershed outlet. As a result, soils along concentrated flow paths eventually become saturated and produce overland flow. Although there may be some loss due to re-infiltration, the effect on the overall hydrograph is minimal.

The effect of the two proposed landuse scenarios on peak discharge decreased relative to the baseline simulation. Peak discharges were decreased by 37% and 75% for Case 1 and Case 2, respectively, compared to the baseline simulation. A smaller but noticeable delay in time to peak also occurred. The percentage of runoff to total rainfall volume decreased for Case 1 and Case 2 with an associated increase in infiltration volume.

6.3 Model Calibration and Verification

Before any model results become useful, it is important to ensure the model provides accurate and reliable results. The accuracy and reliability of a model is usually tested in two stages, calibration and verification. Calibration is performed to ensure the model inputs are reasonable and requires a past event where rainfall and stream discharge data are available. The hydrologic response is simulated for the known rainfall-runoff event and compared to the observed data to determine if the estimated results are within a predetermined range (*e.g.*, 2% - 3%). If they are not within the predetermined range, parameter values are adjusted until an acceptable match is made at

Reproduced with permission of the copyright owner. Further reproduction prohibited without permission.

which time, the model is then considered to be calibrated (Bedient and Huber, 1992; Morgan, 1988; Parker *et al.*, 1995).

Verification is performed to ensure the models outputs are reasonable. Similar to model calibration, verification requires rainfall and stream discharge data from a past event that is independent from the calibration data. The hydrologic response is simulated for the known verification rainfall-runoff event and compared to the observed data. If the estimated and observed data are within a predetermined range, the model is considered to be verified. Model verification should be conducted for several storms. If further adjustments to the model parameters are required it is important to note that the verification data becomes part of the calibration dataset and a new dataset is required for the verification (Bedient and Huber, 1992; Morgan, 1988; Parker *et al.*, 1995).

For this study, no model calibration or verification was performed due to inadequate rainfall data and the lack of stream discharge data.

Reproduced with permission of the copyright owner. Further reproduction prohibited without permission.

CHAPTER 7: DISCUSSION

7.1 Database

The integration of data from a variety of sources resulted in problems with proper co-registration of spatial features when the data was merged into one database. Both the soil quality map and GPS data coordinates were found to be systematically shifted (by various amounts) when compared to the topographic map sheet data. As it is difficult to ascertain where the error exists (topographic map sheets, soils quality map or GPS data), the topographic base map was assumed to be correct and all data was adjusted to match the Ghana survey map sheet. The Ghana survey map sheets were selected because of its larger scale.

Historical meteorological data at the Bawku-Manga station was collected on a daily basis. For single event modelling purposes this data was inadequate since it did not provide information on rainfall duration or rainfall intensity. Since the watershed selected for this study was ungauged, no stream discharge data was available and model calibration could be not performed. Daily stream discharge data are currently available from the Tamne watershed adjacent to the study area, but was inadequate for single event hydrological modelling.

To delineate correctly the watershed from the DEM, supplementary elevation data along roads is required. Due to the relatively low relief of the area, the roads created an artificial watershed boundary. Such small changes in elevation were not captured on the Ghana Survey maps at the 1:50,000 scale and resulted in minor errors in the delineation of the watershed boundary. For modelling of larger watersheds, the 15.24 m (50 ft) contour data used to generate the DEM would be sufficient.

The Ghana Survey map sheet and soil quality maps represented conditions at the time they were produced. Updating obvious features, such as roads and streams, was not

Reproduced with permission of the copyright owner. Further reproduction prohibited without permission.

difficult due to the availability of satellite imagery. A more difficult task was evaluating changes to the soils quality map. As discussed earlier, the increase in land degradation within the area has been well documented. Thus, it can be expected that the soils quality map may not properly reflect current conditions and soil properties, such as infiltration, may have changed since the map was produced.

7.2 Model Sensitivity

The model's output was sensitive to all parameters tested. Although an increase in grid cell size from 75 m to 100 m and 200 m did not substantially alter the general morphological characteristics of the watershed (*i.e.*, area, perimeter, slope), a considerable decrease in peak discharges occurred as the grid cell size decreased. Since the study area's topography is not very complex, the increase in grid cell size did not have a large impact on watershed morphology. This may not be the case for more complex watersheds where grid cell size may have a greater impact. It can be expected that smaller grid cell sizes provide better representation of watershed characteristics. Furthermore, it is important to note that the data accuracy will not increase if the grid cell size decreases below the original resolution of the original data. The differences in peak discharge indicated that care should be taken when selecting the correct grid cell size. However, for this study, an optimal grid cell size was not determined in this study because calibration data was not available.

Under the 30 mm/hr rain intensity rainfall event, clay, sandy clay and silty clay all produced variable rates of surface runoff. There was no substantial runoff that occurred with regards to the other soil textures examined. The Green and Ampt infiltration parameters were estimated using the soil texture approach by Rawls *et al.* (1983b). Detailed field studies will be required to validate these values or values should be adjusted to account for changes in soil porosity, organic matter, rock content and surface soil crusting. Infiltration rates may be significantly reduced by surface crusting which may develop from the impact of rain drops onto the soil surface. In Mali, for example, the infiltration capacity of a sandy soil ranges from 100 mm to 200 mm but may be reduced to 10 mm when a surface crust has developed (Morgan, 1988). In

Reproduced with permission of the copyright owner. Further reproduction prohibited without permission.

addition, with the alternating wet and dry season, soils in the study area experience intense leaching of the top soils which results in hardening of the soils and the formation of hardpans, which reduce infiltration rates (Dept. of Geography, 1992).

Manning's n values provided a measure of surface friction that controlled the flow velocity of the surface runoff. With increasing Manning's n values, peak discharges decreased with corresponding delayed peak times. Even though infiltration was neglected in the sensitivity analysis, the Manning's n values also determined the length of the time the surface runoff remains on the surface which influences the volume of water that can be infiltrated into the soil. Classified satellite imagery provided a current description of landuse within the area but the Manning n value selected to represent the landuse requires careful consideration. Further research would be required to establish appropriate values for the region which better reflect landuse and soil conditions, such as cross contour furrow formation used in cultivation.

7.3 Landuse Scenarios

The impact of two proposed landuse scenarios on the watersheds hydrologic response illustrated the application of r.hydro.CASC2D for landuse planning. The impact of alternative landuse strategies directed at increasing the vegetative cover was found to decrease the peak discharges and delayed peak times relative to the baseline condition. Further studies will be required to determine if the differences reported here are significant.

Agriculture is the primary landuse within the study area with crops grown on a subsistence level. Traditional farming systems, involving shifting cultivation and long fallow periods, has been replaced by continuous cropping involving shorter fallow periods due to food pressures from the rapid growth in population within the area. Agriculture is considered to be the major factor contributing to the problem of land degradation in the Upper North East region (Dept. of Geography, 1992).

The proposed landuse scenarios selected for this study illustrated two possible rehabilitation strategies for improving the poor environmental conditions found within the study area. Low residue crops, such as groundnuts and beans are extensively grown

Reproduced with permission of the copyright owner. Further reproduction prohibited without permission.

in the area. For Case 1, a shift in agriculture crops from groundnuts and beans to corn and millet was proposed. This would help to increase ground cover but still maintain the area under agriculture production. Removal of crop residue after harvest for fodder and fuel, and free range grazing of cattle should be discouraged in an effort to maintain a surface cover after harvest (Quashie-Sam, pers. comm., 1996).

The impact of shifting areas under groundnuts and bean production on soils classified as non-arable to range land and crop tree production was demonstrated in Case 2. This scenario provides a multi-purpose approach to land rehabilitation by providing grazing areas for cattle and a means for generating income for farmers from the cash crop trees.

The proposed landuse scenarios illustrate two possible options available in an effort to increase ground vegetation. A variety of other options may be explored. For example, utilizing the channel routing option in r.hydro.CASC2D, the impact of channel rehabilitation efforts may be examined. Past programs designed to eradicate the tse-tse fly breeding grounds resulted in the removal of vegetation along stream banks and caused severe stream bank erosion along many of the stream channels (Quashie-Sam, pers. comm., 1996). Scenarios may be investigated that involve establishment of grasses and trees along waterways in an effort to provide tree cover and reduce stream bank erosion.

With continued pressure on agriculture lands from a growing population, a sustainable agriculture system is required. Another proposed landuse scenario may be directed at introducing an agroforestry system within the watershed. Due to continuous cropping and reduced fallow periods, soil fertility levels within the Upper North East region have declined. Agroforestry is a system that incorporates agriculture and tree crops, animals and/or forest plants which increases overall production per unit land. A successful agroforestry system ensures soil conservation, micro-climate and water conservation and provides economic and socio-economic benefits (Agyeman and Brookman-Amissah, 1987).

Possible agroforestry systems that may be explored include the establishment of:

1) woodlots for poles and firewood production;

Reproduced with permission of the copyright owner. Further reproduction prohibited without permission.

2) field boundaries comprised of tree and herbaceous legumes; or
3) trees and herbaceous legumes to improve soil fertility and to provide livestock fodder.

7.4 Study Limitations

The major limitation to this study was lack of data and was an important issue that must be addressed if further research is to be conducted. Although satellite imagery provided an excellent means of updating some features on outdated maps, the lack of current material for this project was considerable. Lack of appropriate meteorological data was also a major problem.

One of the difficulties of utilizing satellite imagery is acquiring cloud free imagery. For this study, dry season imagery was used because cloud free imagery was not available during the rainy season. Radar imagery may be useful since clouds are transparent to microwave radiation and images can therefore be collected during the rainy months and incorporated with the dry season data. Using a variety of image merging techniques landuse classifications from satellite imagery can be improved. In addition to landuse classification, remote sensing offers a method to collect rainfall, soil moisture and evapotranspiration information used by r.hydro.CASC2D.

Furthermore, the lack of calibration and model verification due to inadequate rainfall data and the lack of stream discharge data prevents any meaningful measure of the model's performance.

Reproduced with permission of the copyright owner. Further reproduction prohibited without permission.

CHAPTER 8: CONCLUSIONS AND RECOMMENDATIONS

8.1 Conclusions

This study was initiated to investigate the use of a physical based hydrological model in a semi-arid environment and illustrated its application to landuse planning. The generation of the required database utilizing GIS, remote sensing and GPS technologies was demonstrated and was found to be an efficient method in the data capture and management of the model inputs. Problems associated with merging data from different sources and scales were discussed. Areas where data were inadequate were identified: 1) outdated maps; and 2) inadequate meteorological data.

An important component in this study was the compilation of the database used to describe the required spatial and non-spatial watershed characteristics. The initial database based on 1:50,000 scale Survey of Ghana topographical map sheet (1964) provided the initial topography and drainage data used to generate the DEM and for rectification of the SPOT satellite image. Supplementary information such as roads and villages were also obtained from the map sheet. Soils data were obtained from soil quality maps produced at a 1:250,000 scale by Adu (1969). A classified SPOT XS satellite imagery provided a current description of landuse practices. In addition to providing landuse data, the satellite image was important in updating the topographical map sheets (*e.g.*, correct shifting streams) and in verifying the accuracy of all spatial information (*e.g.*, GPS data) to insure all data was co-registered.

The GIS was an important tool for the preparation of the required database for the model used in this study. The advantage of a GIS-based model was illustrated with the production of output maps describing the spatial distribution of surface flow depths which was helpful in assessing the accuracy of the DEM. In addition to the surface flow

Reproduced with permission of the copyright owner. Further reproduction prohibited without permission.

depth maps, cumulative infiltration depth maps and infiltration rate maps may also be generated and compared to examine the spatial effects of various landuse scenarios which may help to identify areas requiring further attention.

The sensitivity analysis illustrated the model's ability to reflect changes in selected model parameters. Careful consideration was required when selecting the grid cell size, soil infiltration parameters and Manning's n values.

Increasing land degradation within the study area required a better understanding of the impact proposed changes in landuse have on the watershed's hydrologic response. Simulation of two proposed landuse scenarios demonstrated the impact proposed changes would have on the hydrologic response of the area.

8.2 Recommendations for Future Research

The following is a summary of the areas that require further research with regards to watershed modelling in Ghana.

1) Collection of rainfall and stream discharge data recorded at an appropriate temporal resolution (*i.e.*, minutes);
2) Verification of published values (*i.e.*, Green and Ampt soil hydraulic parameters and Manning's n values) to determine if values are appropriate for conditions found in Ghana;
3) Investigate the potential of remote sensing technologies in determining some of the required input parameters. This may include the use of radar imagery for collecting rainfall data or determining soil moisture conditions; and
4) Model calibration and verification will be required. This step is essential and can only be carried out when the appropriate rainfall and discharge data have been collected.

Reproduced with permission of the copyright owner. Further reproduction prohibited without permission.

LITERATURE CITED

Acheampong, P.K. 1988. Water balance analysis for Ghana. Geography. 73(1): 125-131.

Adu. S.V. 1969. Soils of the Navrongo-Bawku area. Upper Region. Ghana. Soil Research Institute. Council for Scientific and Industrial Research Memoir No. 5, Kumasi. 95 pp.

Agurgo, F.B. 1992. Remote sensing applications for forest management *in* Ghana. pp. 22-23 *in* Proc. GIS for Environmental Resource Management: Workshop on Geographic Information Systems,. Environmental Protection Council Accra, 9-10 April. 34 pp.

Agyeman, V.K. and J. Brookman-Amissah. 1987. Agroforestry as a sustainable agricultural practice in Ghana. pp. 131-140 *in* Proc. National conference on resource conservation for Ghana's sustainable development. April 28-30, 1987, Accra, Ghana. Environmental Protection Council. Vol. 2. 307 pp.

Amamoo-Otchere, E. 1990. The utilization of SPOT satellite XS imageries for the characterization of inland valleys of the Northern Region of Ghana: Initial evaluation. Groupement pour le Développement de la Télédétection Aérospatiale: Ecole Nationale des Sciences Géographiques. CETEL 1990-1991. 36 pp.

Amoyaw-Osei, Y. 1992. Applying GIS in basin management pp. 25-26 *in* Proc. GIS for Environmental Resource Management: Workshop on Geographic Information Systems, Environmental Protection Council, Accra, 9-10 April. 34 pp.

Beasley, D. B., and L.F. Huggins. 1981. ANSWERS Users Manual. EPA-905/9-82-01. U.S. Environmental Protection Agency Region V, Chicago, IL. 55 pp.

Becker, A. and P. Serban. 1990. Hydrological models for water resources system design and operation. World Meteorological Organization: Operational Hydrology Report No. 34. 80 pp.

Bedient, P.H. and W.C. Huber. 1992. Hydrology and Floodplain Analysis. Addison-Wesley. Reading, Massachusetts. 692 pp.

Bonsu, M. and H.B. Obeng. 1979. Final project report on the north-east Ghana savannah research project: Cultivation practices. Soil Research Institute, Kwadaso, Kumasi. 11 pp.

Bulley, H.N. 1996. Assessment of landcover changes and hydrologic response of Tamne River Basin. Msc (Forestry) Thesis. Faculty of Forestry, Lakehead University, Thunder Bay, Ontario, Canada. 137 pp.

Reproduced with permission of the copyright owner. Further reproduction prohibited without permission.

Brakensiek, D.L. and W.J. Rawls. 1983. Agriculture management effects on soil water processes Part II: Green and Ampt parameters for crusting soils. Trans. of the ASAE. 26(6):1753-1757.

Cline, T.J., Molinas, A., and P.Y. Julien. 1989. An Auto-CAD-based watershed information system for the hydrologic model HEC-1. Water Resources Bulletin. 25(3):641-652.

Connors, K.F., T.W. Gardner, and G.W. Petersen. 1985. Digital analysis of the hydrologic components of watersheds using simulated SPOT imagery. pp. 355-365 *in* Hydrologic Applications of Space Technology: Proc. of the Cocoa Beach Workshop, Florida, August. IAHS Publ. no. 160.

Danso, J.K. 1992. Application of Geographic Information System in pollution control, pp 24 *in*. Proc. GIS for Environmental Resource Management: Workshop on Geographic Information Systems. Environmental Protection Council Accra, 9-10 April. 34 pp.

Department of Geography and Resource Development. 1992. A socio-economic survey in the Upper East Region with reference to drought and desertification control in Ghana: Final report submitted to the Environmental Protection Council of Ghana, University of Ghana, Legon. 189 pp.

DeVantier, B.A and A.D. Feldman. 1993. Review of GIS application in hydrologic modelling. Journal of Water Resources Planning and Management. 119(2):246-261.

Doe, W.W. 1992. Simulation of the spatial and temporal effects of army maneuvers on watershed response. PhD. Dissertation, Civil Engineering Dept., Colorado State University, Fort Collins, Colarado. 301 pp.

Engel, B.A., R. Srinivasan and C. Rewerts. 1992. Modeling erosion and surface water quality. pp. 107-116. *in* Proc. 7th Annual GRASS Users Conference, National Park Service Technical report NPS/NRG15D/NRTR-93/13, Lakewood, Colorado.

ERDAS. 1991. Field Guide. ERDAS Atlanta.

ESRI. 1992. Understanding GIS: The Arc/Info method. Environmental System Research Institute, Inc. Redlands, CA.

Gyamfi-Aidoo, J. 1987. Application of GIS to the assessment of land degradation and associated hazards in the Upper East Region of Ghana. pp. 487-497 *in* Proc. GIS'87-San Francisco: Second Annual International Conference, Exhibits and Workshops on Geographic Information Systems. San Francisco, California. October 26-30. 756 pp.

Reproduced with permission of the copyright owner. Further reproduction prohibited without permission.

Greene, R.G and J.F. Cruise. 1985. Urban watershed modeling using geographic information system. Journal of Water Resources, Planning and Management. 121(4):318-325.

Haan, C.T., B.J. Barfield and J.C. Hayes. 1994. Design Hydrology and Sedimentology for small catchments. Academic Press. 588. pp.

Hill, J. M., V. P. Singh, and H. Aminian, 1987. A computerized data base for flood prediction modeling. Water Resources Bulletin. 23:21-27.

Horton, R. E. 1940. Approach toward a physical interpretation of infiltration capacity. Soil Sci. Soc. Am. Proc. 5:339-417.

Hutchinson, M.F. 1988. Calculation of hydrologically sound digital elevation models. pp. 117-133 *in* Proc. Third International Symposium on Spatial Data Handling, NSW: International Geographic Union. Sydney, Ohio.

Hutchinson, M.F. 1989. A new procedure for griding elevation and stream line data with automatic removal of spurious pits. J. of Hydrol. 106: 211-232.

Issaka, F. 1992. Opening address. pp. 6 *in* Proc GIS for environmental resources. Proc. workshop on geographic information systems. Environmental Protection Council. Accra, 9-10 April. 34pp.

James, W.P. and K.W. Kim. 1990. A distributed dynamic watershed model. Water Resources Bulletin. 26(4):587-596.

Johnson, B.E., N.K. Raphelt and J.C. Willis. 1993. Verification of hydrologic modeling Systems. pp 9-20. *in* Proc. Federal Water Agency Workshop on Hydrologic Modeling Demands for the 90's, USGS Water Resources Investigations Report 93-4018, June 6-9, Sec 8.

Julien, P.Y. and F.L. Saghafian. 1991. A two-dimensional watershed rainfall-runoff model. Civil Engr. Report. CER90-91PYJ-BS-12, Dept of Civil Engineering. Colorado State University, Fort Collins, Colorado. 63pp.

Julien, P.Y., B. Saghafian, F.L. Ogden. 1995. Raster-based hydrologic modeling of spatially-varied surface runoff. Water Resources Bulletin. 31(3):523-536.

Kendie, S.B. 1995. The environmental dimensions of structural adjustments programs: missing links to sustaining development. Singapore J. of Trop. Geogr. 16(1):42-57.

Kuittinen, R. 1992. Remote Sensing for hydrology progress and prospects. World Meteorological Organization: Operational Hydrology Report No. 36. 55pp.

Reproduced with permission of the copyright owner. Further reproduction prohibited without permission.

Lillesand, T.M. and R.W. Kiefer. 1994. Remote sensing and image interpretation, 3rd edition. John Wiley and Sons, New York. 750 pp.

Morgan, R.P.C. 1988. Soil erosion and conservation. English Language Book Society, Longman, Hong Kong. 298 pp.

Mackey, B.G., D.W. McKenney, C.A. Widdifield, R.A. Sims, K. Lawrence and N. Szcyrek. 1994. A digital elevation model of Ontario. Nat. Resour. Can., Canadian Forest Service. Sault Ste. Marie, Ont. NODA/NFP Tech. Rep. TR-6. 31 pp.

Mazion, E. (Jr.) 1994. Computational discretization effect on rainfall-runoff simulation. Journal of Water Resources, Planning and Management. 120(5): 715-734.

Moore, I.D., R.B. Grayson and A.R. Ladson. 1991. Digital terrain modelling: A review of hydrological, geomorphological, and biological applications. Hydrological Processes. 5(1): 3-30.

Ofori-Sarpong, E. 1985. The nature of rainfall and soil moisture in the northeastern part of Ghana during the 1975-1977 drought. Geogr. Ann. 67A(3-4):177-186.

Ofori-Sarpong, E. 1986. The 1981-1983 drought in Ghana. Singapore J. of Trop. Geogr. 7(2):108-126.

Ogden, F.L., and B. Saghafian. (1996). r.hydro.CASC2D reference manual. ftp://moon.cecer.army.mil/pub/grass/outgoing/Raster/r.hydro.CASC2D_1.01.tar.Z (June 1, 1996).

Panda, J.C., S.A. Nielsen and I.D Moore. 1988. A hydrologic model for small agriculture catchments in the semiarid tropics. Proc. ASAE International Symposium on Modeling, Forest, and Rangeland Hydrology, Hyatt Regency Hotel, Chicago. IL., Dec. 12-13, 1988.

Parker, M., J.G. Tompson, R.R. Reynolds, Jr. and M.D. Smith. 1995. Use and misuse of complex models: Examples from water demand management. Water Resources Bulletin. 31(2): 257-263.

Pimentel, D. 1993. World soil erosion and conservation. Cambridge University Press. Cambridge, New York. 349 pp.

Ponce, V.M. 1989. Engineering hydrology principles and practices. Prentice Hall. New Jersey. 640 pp.

Quashi-Sam, S.J. 1996. Pers. comm. Institute of Renewable Natural Resources, University of Science and Technology. Kumasi, Ghana.

Reproduced with permission of the copyright owner. Further reproduction prohibited without permission.

Rango, A. 1985. Assessment of remote sensing input to hydrologic models. Water Resources Bulletin. 21(3):423-432.

Rawls, W.J.,D.L. Brakensiek and N. Miller. 1983a. Green-Ampt infiltration parameters from soils data. J. Hydraulic Eng., Proc. Am. Soc. Civil Eng. 109(1):62-70.

Rawls, W.J., D.L. Brakensiek and B. Soni. 1983b. Agriculture management effects on soil water processes Part I: Soil water retention and Green and Ampt infiltration parameters. Trans. of the ASAE 26(6):1747-1752.

Rewerts, C.C. and B.A. Engel. 1991. ANSWERS on GRASS: integrating a watershed simulation with a GIS. ASAE Paper 91-2621, American Society of Agriculture Engineers. St. Joseph, Michigan. 8pp.

Runesson, U.T. 1996. Pers. comm. Lakehead University, Thunder Bay, Ontario.

Savabi, M.R., D.C. Flanagan, B. Hebel and B.A. Engel. 1995. Application of WEPP and GIS-GRASS to a small watershed in Indiana. Journal of Soil and Water Conservation. 50(5):477-483.

Saghafian, B. 1992. Hydrologic analysis of watershed response to spatially varied infiltration. Ph.D. Dissertation, Colorado State University, Department of Civil Engineering, Fort Collins, Colorado. 215pp.

Stuebe, M.M, and D.M., Johnston. 1990. Runoff volume estimate using GIS techniques. Water Resources Bulletin. 26(4):611-620.

Sutherland, R. 1994. Teaching the hydrologic and Geomorphic significance of drainage basins and discharge in physical geography. Journal of Geography. 93(2):80-95.

Suwanwerakamtorn, R. 1994. GIS and hydrologic modeling for the management of small watersheds. ITC Journal. 4:343-348.

UN. 1991. United Nations conference on environment and development (UNCED): Environment and development in Ghana, Ghana National Report. Geneva. 70pp.

Vieux. B.E., and N. Gauer. 1994. Finite-element modeling of storm water runoff using GRASS GIS. Microcomputers in Civil Engineering 9(4):263-270.

Warwick, J.J., and S.J. Haness. 1994. Efficacy of ARC/INFO GIS applications to hydrologic modeling. Journal of Water Resources Planning and Management. 120(3):366-381.

Reproduced with permission of the copyright owner. Further reproduction prohibited without permission.

White, D., 1988. Grid based application of runoff curve numbers. Journal of the Water Resources Planning and Management Division. 114:601-612.

Wolfe, M.L. and C.M.U. Neale. 1988. Input data development for a distributed parameter hydrologic model (FESHM). pp. 462-469 *in* Proc. ASAE International Symposium on Modeling, Forest, and Rangeland Hydrology, Hyatt Regency Hotel, Chicago. IL., Dec. 12-13, 1988.

Wu, R.S. and D.A. Haith. 1993. Land use, climate, and water supply. Journal of Water Resources, Planning and Management. 119(6):685-704.

Young, R.A., C.A. Onstad, D.D. Bosch, and W.P Anderson. 1987. AGNPS, Agriculture Non-Point Source Pollution Model: A watershed analysis tool. U.S. Dept. of Agric., Conservation Research Report 35.

Reproduced with permission of the copyright owner. Further reproduction prohibited without permission.

APPENDIX 1

Average Green and Ampt parameters and Manning's n values

Reproduced with permission of the copyright owner. Further reproduction prohibited without permission.

Table A1.1. Average Green and Ampt parameters for various soil textures (from Rawls *et al.*, 1983).

Soil Texture	Total Porosity ϕ	Effective Porosity θ_e	Wetting Front Capillary Pressure H_f (cm)	Hydraulic Conductivity K (cm/hr)
Sand	0.437	0.417	4.05	11.78
Loamy Sand	0.437	0.401	6.13	2.99
Sandy Loam	0.453	0.412	11.01	1.09
Loam	0.463	0.434	8.89	0.34
Silt Loam	0.501	0.486	16.68	0.65
Sandy Clay Loam	0.398	0.330	21.85	0.15
Clay Loam	0.464	0.309	20.88	0.10
Silty Clay Loam	0.471	0.432	27.30	0.10
Sandy Clay	0.430	0.321	23.90	0.06
Silty Clay	0.479	0.423	29.22	0.05
Clay	0.475	0.385	31.63	0.03

Reproduced with permission of the copyright owner. Further reproduction prohibited without permission.

Table A.1.2. Manning's n values for overland flow (from Haan *et al.*, 1994).

Surface type	n Value
Smooth surfaces (concrete, asphalt, or bare soil)	0.011
Fallow (no residue)	0.05
Cultivated soils	
Residue cover ≤20%	0.06
Residue cover >20%	0.17
Grass	
Short grass prairie	0.15
Dense grasses	0.24
Range (natural)	0.13
Woods	
Light underbrush	0.40
Dense underbrush	0.80

Reproduced with permission of the copyright owner. Further reproduction prohibited without permission.

APPENDIX 2

Command Line Description for r.hydro.CASC2D

Reproduced with permission of the copyright owner. Further reproduction prohibited without permission.

Command line syntax for the r.hydro.CASC2D model (from Saghafian and Ogden, 1996):

SYNOPSIS: r.hydro.CASC2D, r.hydro.CASC2D help, r.hydro.CASC2D [-toepidbuq] elevation=mapname time_step=value tot_time=value discharge=mapname outlet_east&north&slope=east,north,bedslope rain_duration=value [watershed_mask=mapname] [initial_depth=mapname] [storage_capacity=mapname] [interception_coefficient=mapname] [roughness_map=mapname] [Manning_n=value] [conductivity=mapname] [capillary=mapname] [porosity=mapname] [moisture=mapname] [pore_index=mapname] [residual_sat=mapname] [lake_map=mapname] [lake_elev=mapname] [radar_intensity_map=mapname] [links_map=mapname] [nodes_map=mapname] [channel_input=mapname] [table_input=mapname] [dis_profile=mapname] [wat_surf_profile=mapname] [hyd_location=mapname] [r_gage_file=mapname] [unif_rain_int=value] [num_of_raingages=value] [gage_time_step=value] [radar_time_step=value] [write_time_step=value] [unit_el_conv=value] [unit_lake=value] [unit_space=value] [d_thresh=value] [dis_hyd_location=mapname] [depth_map=mapname] [inf_depth_map=mapname] [surf_moist_map=mapname] [rate_of_infil_map=mapname] [dis_rain_map=mapname]

PARAMETERS/OPTIONS: The following input/output parameters/options control complexity of the simulation. Map and file names in square brackets [] are optional. Some maps are mutually exclusive (logical -or-), while some maps require other maps to enable proper function (logical -and-).

INPUT

Topography

elevation=mapname	map of elevation (DEM).
outlet_east&north&slope=value, value,value (comma delimited)	easting, northing, and bed slope at the outlet

Time

time_step=value	computational time step duration in seconds (1 to 30 seconds)
tot_time=value	total simulation time in sec.

Reproduced with permission of the copyright owner. Further reproduction prohibited without permission.

Overland Flow

[Manning_n=value]	spatially uniform Manning's n roughness value for overland flow.
-or-	
[roughness_map=mapname]	spatially varied map of Manning's n roughness coefficient (values in 1000*Manning's n).
[watershed_mask=mapname]	map of watershed boundary (or mask). This option is recommended, as it speeds execution greatly.
[d_thresh=value]	threshold overland depth, in meters, below which overland routing will not be performed (i.e. average depression storage).
[initial_depth=mapname]	map of initial overland (not lakes) depth in mm.

Rainfall

rain_duration=value	total rainfall duration in sec.
[unif_rain_int=value]	spatially uniform rainfall intensity in mm/hr.
-or-	
[r_gage_file=filename]	raingage rainfall input file name (ASCII).
-and-	
[num_of_raingages=value]	number of recording raingages.
-and-	
[gage_time_step=value]	time step (temporal resolution) of recorded raingage data in sec.
-or-	
[radar_intensity_map=mapname]	prefix of time series of maps of radar- (or otherwise-) generated rainfall intensities in mm/hr.
-and-	

Reproduced with permission of the copyright owner. Further reproduction prohibited without permission.

[radar_time_step=value]	time increment between radar- (or otherwise-) generated rainfall maps in sec.
Interception	
[storage_capacity=mapname]	map of vegetation storage capacity in tenths of mm.
-and-	
[interception_coefficient]	map of interception coefficient (values in 1000*actual coefficient).
Infiltration	
[conductivity=mapname]	map of soil saturated hydraulic conductivity in tenths of mm/hr (Req'd for G&A and Redist).
[capillary=mapname]	map of soil capillary pressure head at the wetting front in tenths of mm (Req'd for G&A and Redist).
[porosity=mapname]	map of soil effective porosity (values in 1000*porosity) (Req'd for G&A and Redist).
[moisture=mapname]	map of initial soil moisture (values in 1000*moisture) (Req'd for G&A and Redist).
[pore_index=mapname]	map of soil pore-size distribution index (Brooks & Corey lambda) in 1000*index (Req'd for Redist).
[residual_sat=mapname]	map of soil residual saturation (values in 1000*residual saturation) (Req'd for Redist).
Lakes	
[lake_map=mapname]	map of lakes categories.
[lake_elev=mapname]	map of lakes initial water surface elevation (also see unit_lake).
Channel Routing	
[channel_input=filename]	channel input data file name (ASCII), required for explicit (EX) and implicit (IM) channel routing methods.

Reproduced with permission of the copyright owner. Further reproduction prohibited without permission.

[links_map=mapname]	map of channel network link numbers. (EX & IM)
[nodes_map=mapname]	map of channel network node numbers. (EX & IM)
[table_input=filename]	look-up table file for links with breakpoint cross section, link type 8, (ASCII) (IM)
[dis_profile=filename]	channel initial discharge profile file name (ASCII). (IM)
[wat_surf_profile=filename]	channel initial water surface profile file name (ASCII). (IM)
[hyd_location=filename]	file name containing link and node numbers of internal locations where discharge hydrographs are to be saved (ASCII).

Units

[unit_el_conv=value]	unit conversion factor by which the values in elevation must be DIVIDED to convert them into meters.
[unit_lake=value]	unit conversion factor by which the values in lake surface elevation map must be DIVIDED to convert them into meters.
[unit_space=value]	unit conversion factor by which all region easting and northing values must be DIVIDED to convert them into meters.

Output

discharge=filename	outlet hydrograph file name (ASCII).
[dis_hyd_location=filename]	output file name for discharge hydrograph at internal locations (ASCII)
[write_time_step=value]	time increment for writing output raster maps in seconds.

-and-

Reproduced with permission of the copyright owner. Further reproduction prohibited without permission.

[depth_map=mapname]	output maps of surface depth in mm.
[inf_depth_map=mapname]	output maps of cumulative infiltration depth in tenths of mm.
[surf_moist_map=mapname]	output maps of surface soil moisture in number of fractions of a thousand.
[rate_of_infil_map=mapname]	output maps of infiltration rate in mm/hr.
[dis_rain_map=mapname]	output maps of distributed rainfall intensity in mm.

FLAGS: There are several flags whose utility is driven by data availability and/or user's choice.

-t spatially interpolates raingage rainfall intensities using Thiessen polygon technique. The default technique uses inverse-distance-squared proportionality for interpolation of rainfall intensity over space.

-o routes edge-accumulated overland flow out of active region (ONLY when no mask is specified). Often the surface water accumulated at the edges of the current region creates severe backwater effects and may limit the use of longer computational time steps.

-e performs one-dimensional explicit finite difference channel routing. May be suitable for low- to medium-intensity rainstorms over small arid and semi-arid watersheds with no base flow discharge. This option often limits the computational time step to small values (<10 seconds). Channel bed smoothing is recommended to eliminate adverse slopes. No hydraulic structures, except reservoir spillways, can be simulated.

-p assumes uniform channel geometry in each link (requires -e option). If this option is chosen, the channel input file (channel_input) must have only one line per fluvial link rather than the default of one line per node.

-I performs Preissmann double sweep implicit channel routing. Particularly suitable for watersheds with some base flow to avoid dry-bed condition with channel slopes less than 1%. Supercritical slopes cannot be handled; a warning message will be printed if supercritical flow is encountered.

-b initializes the channel depth and discharge files (similar to -d, requires -i option) using the standard step backwater method. This option must be used with -i flag and replaces -d option to write "dis_profile" and "wat_surf_profile" files. At present, only link types 1, 2, and 8 may exist in the channel network.

Reproduced with permission of the copyright owner. Further reproduction prohibited without permission.

-d performs channel initialization for implicit routing (similar to -b, requires -i option) by flooding the entire channel network with a horizontal water surface and draining down to normal depth using a y(t) outlet boundary condition (similar to -b). It is essential for implicit channel routing technique that a minimum initial base flow discharge exist in the channels and also the corresponding initial water surface profile at each node in the channel network have a realistic value. When the depth at the outlet reaches normal depth, the values of depth and discharge at each node is written to "dis_profile" and "wat_surf_profile" files for use in start up of actual simulations. With this option no other component of the model is executed; only the implicit channel routing is performed to create initial depth and discharge files necessary for start up of actual simulations.

-u writes discharges in cubic feet per second (cfs) and volumes in cubic feet in "discharge" file. The internal calculations are all in SI units regardless of this flag. The default SI unit prints the discharges in cubic meters per second (cms) and volumes in cubic meters (m3).

-q quietly skips printing iteration, time, and discharge values to the screen. No status report is printed.

Reproduced with permission of the copyright owner. Further reproduction prohibited without permission.

APPENDIX 3

Green and Ampt Soil Texture Graphs

Reproduced with permission of the copyright owner. Further reproduction prohibited without permission.

Based on soil texture, organic matter and porosity, the Green and Ampt soil infiltration parameters were estimated from soil texture charts defined by Rawls *et al.* (1983). Soil texture charts for soils with a base porosity condition (0% porosity change) and 0.5% organic matter content are presented in Figure A.3.1 and A.3.2. Although not shown, additional charts have been defined for increased changes in soil porosity (+10%, 20% and +30% over the base porosity) which results from soil modification from cultivation.

The estimated soil infiltration parameters for a sandy loam soil is illustrated in Figures A.3.1 and A.3.2. Since no soil texture data was available, the centroid of the soil texture class was used.

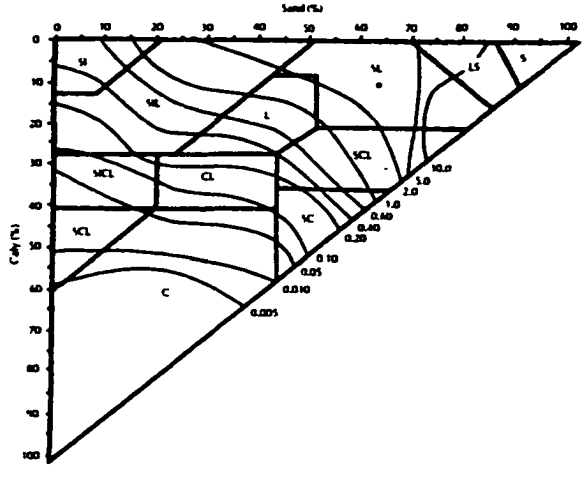

a)

Saturated Soil Conductivity

$K = 3.0$ cm/hr

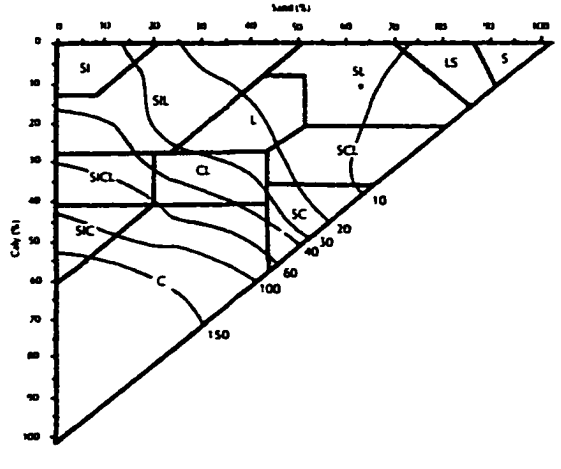

b)

Wetting Front Capillary Pressure

$H_f = 11$ cm

Figure A.3.1. Green and Ampt infiltration parameters for a sandy loam soil a) saturated hydraulic conductivity b) wetting front capillary pressure soil.

Reproduced with permission of the copyright owner. Further reproduction prohibited without permission.

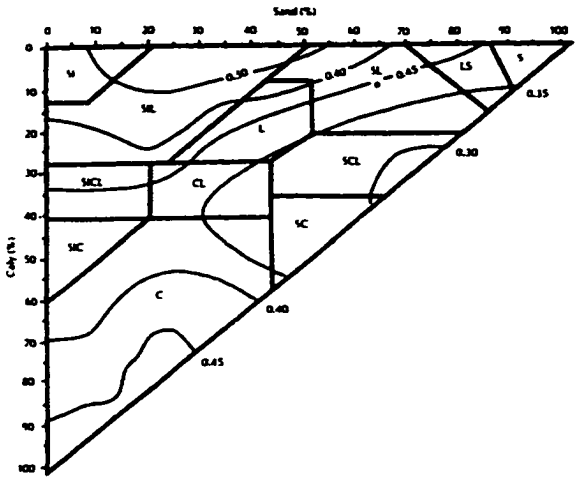

a)

Effective porosity

$\theta = 0.45$

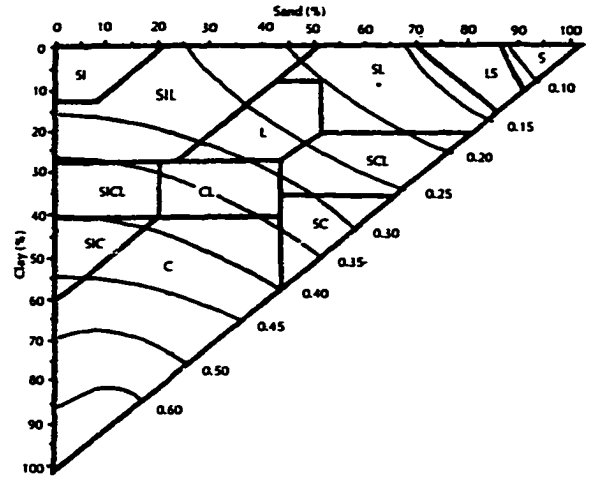

b)

Soil moisture at 1/3 bar (field capacity)

0.18

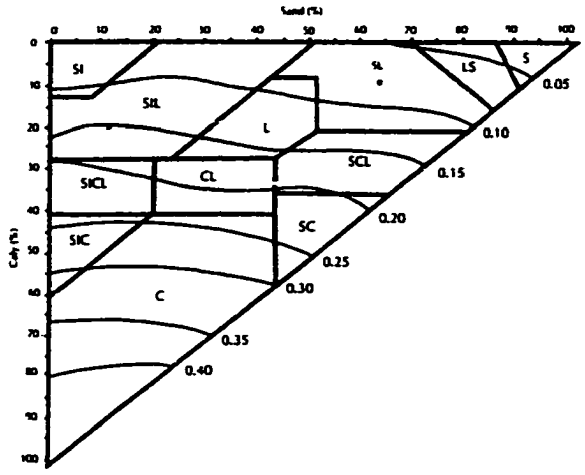

c)

Soil moisture at 15 bar (wilting point)

0.07

Figure A.3.2. Green and Ampt infiltration parameters for a sandy loam soil a) effective porosity b) soil moisture at 1/3 bar c) soil moisture at 15 bar.

Reproduced with permission of the copyright owner. Further reproduction prohibited without permission.

IMAGE EVALUATION TEST TARGET (QA-3)

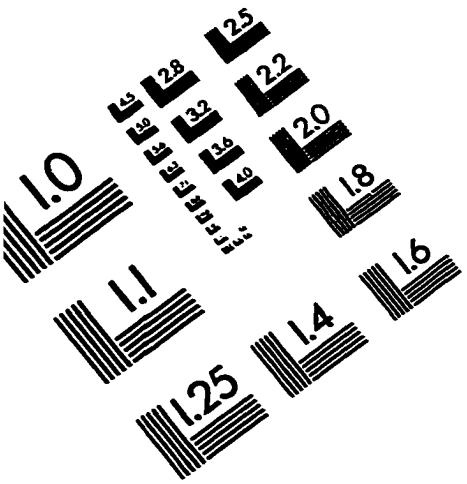

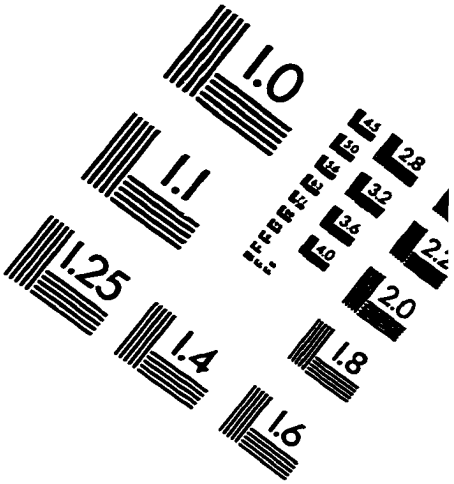

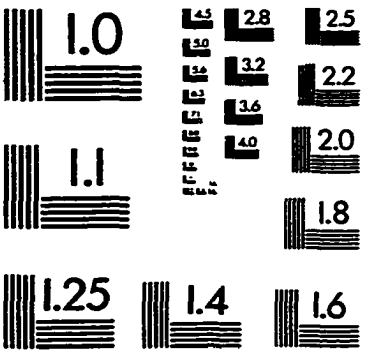

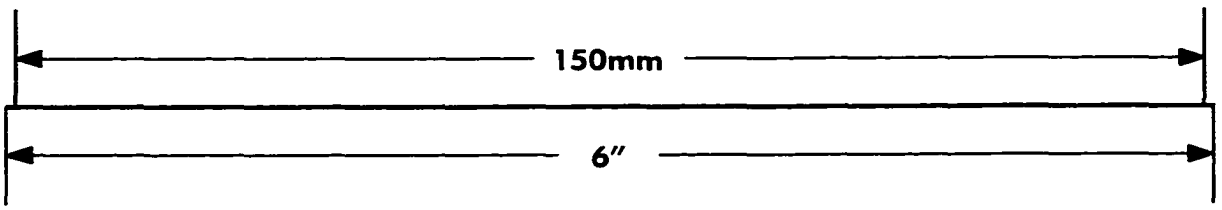

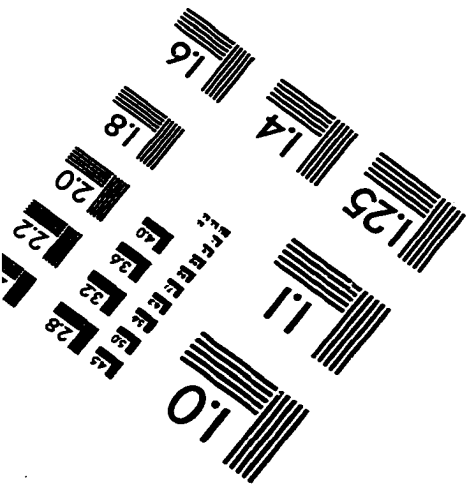

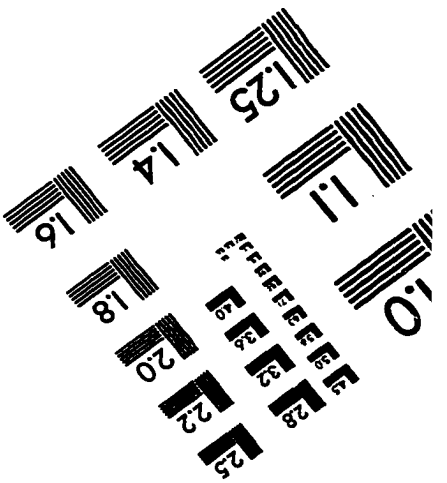

APPLIED IMAGE, Inc
1653 East Main Street
Rochester, NY 14609 USA
Phone: 716/482-0300
Fax: 716/288-5989

© 1993, Applied Image, Inc., All Rights Reserved

Reproduced with permission of the copyright owner. Further reproduction prohibited without permission.